Cooperative Diversity for Inter-Vehicular Communications

by

Muhammad Jawwad Hussain

A thesis
presented to the University of Waterloo
in fulfillment of the
thesis requirement for the degree of
Master of Applied Science
in
Electrical and Computer Engineering
Waterloo, Ontario, Canada

AUTHOR'S DECLARATION

I hereby declare that I am the sole author of this thesis. This is a true copy of the thesis, including any required final revisions, as accepted by my examiners.

I understand that my thesis may be made electronically available to the public.

Abstract

Recent technological advances and pervasiveness of wireless communication devices have offered novel and promising solutions to the road safety problem and on-the-go entertainment. One such solution is the Inter-Vehicular Communications (IVC) where vehicles cooperate in receiving and delivering the messages to each other, establishing a decentralized communication system.

The communication between vehicles can be made more effective and reliable at the physical layer by using the concept of space-time coding (STC). STC demonstrated that the deployment of multiple antennas at the transmitter allows for simultaneous increase in throughput and reliability because of the additional degree of freedom offered by the spatial dimension of the wireless. However, the use of multiple antenna at the receiver is not feasible because of the size and power limitations. Cooperative diversity, which is also known as user cooperation is ideal to overcome these limitations by introducing a new concept of using the antenna of neighboring node. This technique exploits the broadcast nature of wireless transmissions and creates a virtual (distributed) antenna array through cooperating nodes to realize spatial diversity advantage.

Although there has been a growing literature on cooperative diversity, the current literature is mainly limited to Rayleigh fading channel model which typically assumes a wireless communication scenario with a stationary base station antenna above roof-top level and a mobile station at street level. In this thesis, we investigate cooperative diversity for inter-vehicular communication based on cascaded Rayleigh fading. This channel model provides a realistic description of inter-vehicular channel where two or more independent Rayleigh fading processes are assumed to be generated by independent groups of scatters around the two mobile terminals. We investigate the performance of amplify-and-forward relaying for an inter-vehicular cooperative scheme assisted by either a road-side access point or another vehicle which acts as a relay. Our diversity analysis reveals that the cooperative scheme is able to extract the full distributed spatial diversity. We further formulate a power allocation problem for the considered scheme to optimize the power allocated to broadcasting and relaying phases. Performance gains up to 3 dB are obtained through optimum power allocation depending on the relay location.

Acknowledgements

Although I am indeed the sole author of this thesis, as customarily declared in the beginning, I am surely not the sole contributor! So many people have contributed to my thesis, to my education, and to my life, and it is now my great pleasure to take this opportunity to thank them.

I am grateful to Dr. Murat Uysal for enlightening discussions, moral support, and advices in my career development/search. Dr. Murat Uysal extensive contributions to leading edge industrial research have been great assets for me. His tenacity, wisdom, and perseverance have been sources of inspiration and guidance for me. Above all, he understands the contrast between creativity and productivity and he is appreciative of both in scientific inquiries. His infectious optimism and dynamic personality transformed the manner in which I approach challenges in my career. He is an ideal role model for aspiring scientists and academicians.

Dr. Abdul Rahim Ahmad sound judgment and project management skills were instrumental in the successful completion of this thesis. I would like to thank him for his mentoring, support, and encouragement. He has guided and helped me with his extensive knowledge and experience during my research. I thank him for his efforts towards the development of my career and this work..

Special thanks to Dr. Mohamed-Yahia Dabbagh and Dr. Pin-Han Ho, members of the thesis reading committee, for devoting their time out of their busy schedule. I would also like to thank my colleagues Mehboob Fareed, Osama Amin, and Suhail Al-Dharrab , who provided endless source of support and inspiration.

Dedication

To my Much-loved Late Parents

Table of Contents

List of Figures

List of Tables

List of Abbreviations

UMTS	Universal Mobile Telecommunication System
IVC	Inter-vehicular Communications
ITS	Intelligent Transportation Systems
V2V	Vehicle-to-Vehicle communications
V2R	Vehicle-to-Roadside communications
FCC	Federal Communications Commissions
DSRC	Dedicated Short Range Communication
SNR	Signal-to-noise Ratio
AWGN	Additive White Gaussian Noise
CDMA	Code Division Multiple Access
OFDM	Orthogonal Frequency Division Multiplexing
BER	Bit Error Rate
MRC	Maximum Ratio Combining
CSI	Channel State Information
STTCs	Space-time Trellis Codes
STBCs	Space-time Block Codes
MIMO	Multiple Input Multiple Output
TD	Transmit Diversity
RD	Receive Diversity
APA	Access Point Assisted
VA	Vehicular Assisted
EPA	Equal Power Allocation
OPA	Optimum Power Allocation
PEP	Pairwise Error Probability

Chapter 1

Introduction

During the last century, Wireless technologies such as Global System for Mobile communication (GSM), Universal Mobile Telecommunication System (UMTS), Worldwide Interoperability for Microwave Access (WiMAX-802.16), and Bluetooth [1] have revolutionized the way we communicate and exchange data by making services like telephony internet, and multimedia access available at anytime and from almost anywhere. This advancement in information and communication technologies, especially wireless technologies have played a meaningful role in our daily lives enabling many conveniences and raised our daily productivity.

One of the untapped areas where wireless technologies are now making a significant impact is inter-vehicular communications (IVC) [2]. IVC is a crucial component of the intelligent transportation systems (ITSs) which involve the application of advanced information processing, communications, sensor, and control technologies in an integrated manner to improve the functioning of the transportation system. IVC involves vehicle-to-vehicle (V2V) and vehicle-to-road (V2R) communications enabling a vehicle to communicate with other vehicles and sensors/access-points installed along the road. Road safety and traffic flow can be improved if drivers have the ability to predict further down the road and know if a collision has occurred, or if they are approaching a traffic jam. The real-time information transmitted via IVC can also help vehicles at critical points such as blind crossings and entries to highways. Besides these main navigation safety functionalities, potential in-vehicle applications have recently emerged such as audio/video streaming, high-speed internet access, cooperative downloading, multiplayer gaming, and mobile commerce [3] as a result of ever-increasing dependence on internet and multimedia services.

In summary, the potential ability of vehicles to communicate directly via wireless links is opening up a plethora of exciting applications. The main applications of IVC, as summarized by [4], can be categorized into three classes:

Advance driver assistance: Increasing road safety by reducing the number of accidents as well as reducing the impact in case of non-avoidable accidents.

User communications and information services: Offering comfort and business applications to drivers and passengers.

Decentralized floating car data: Improving local traffic flow and efficiency of road traffic.

On the physical layer of IVC, the media used so far includes both infrared and radio waves. The radio waves include VHF, micro, and millimeter waves. Although VHF waves such as 220MHz band have been used because of their long communication distance, the mainstream nowadays is microwaves. The Federal Communications Commission (FCC) approved 75 MHz bandwidth at 5.850- 5.925GHz frequency bands for ITS wireless communications between vehicles and roadside infrastructures, which is also called Dedicated Short Range Communication (DSRC) spectrum [5]. In Japan, 5.8 GHz DSRC was used by company DEMO 2000 [6] and 60 GHz millimeter waves has been tested to evaluate its performance under the hidden terminal situation [10]. In Europe, Chauffeur chose 2.4 GHz at the beginning [7] then they changed it to 5.8 GHz. CarTALK/FleetNet chose UTRA TDD because of the availability of an unlicensed frequency band at 2010-2020 MHz in Europe [4]. It is worth to note that infrared, in spite of its various drawbacks, has been deployed by most projects including PATH [8] and CarTALK, typically for co-operative driving.

DSRC is based on IEEE 802.11p standard for wireless access in vehicular environment. As shown in Figure 1.1, the overall bandwidth is divided into seven frequency channels [9]. The channel time is divided into synchronization intervals with a fix length of 100ms, consisting of a Control Channel (CCH) interval and Service Channel (SCH) interval, each of 50ms. CCH frequency channels can only be used by safety relevant applications and for system control and management purposes. The other six channels are SCHs, mainly supporting the non-safety applications.

Although there has been a growing literature on the networking and application layers in vehicular networks, the relevant literature on the physical layer aspect is sparse. The main challenge facing the deployment of vehicular networks indeed manifests itself as their main advantage, i.e. the lack of infrastructure. This makes recently proposed cooperative diversity [11]-[13] as an ideal physical layer solution for vehicular networks. . In the following three sections, we will briefly summarize the diversity techniques in general and description for cooperative diversity, which will be the main background of our work.

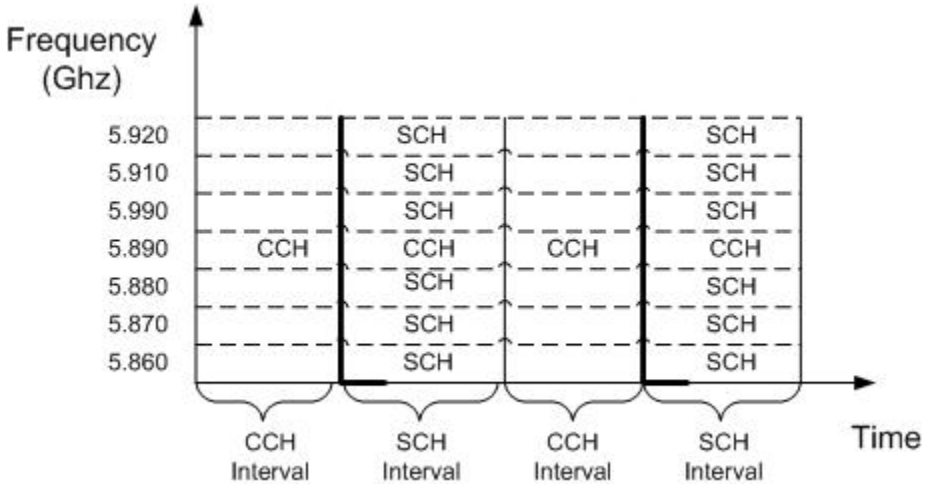

Figure 1.1: Multi-mode channels [9]

1.1 Diversity Techniques

The mobile radio propagation environment places fundamental limitations on the performance of wireless radio systems. There are roughly three complex and independent phenomena that together create a hostile transmission environment: path loss variation with distance, short term (fast) multipath fading and slow log-normal shadowing. The underlying physical principles behind these phenomenons are different. Path loss is due to the decay of electro-magnetic wave intensity in the atmosphere. Multipath fading is due to the constructive and destructive combination of randomly delayed, reflected, scattered, and diffracted signal component. This type of fading is relatively fast and is therefore responsible for short-term signal variations. Slow shadowing is due to the topographical variations along the transmission path.

For a typical mobile wireless channel in urban areas where there is no line of sight propagation and the number of scatters is considerably large, the application of central limit theory indicates that the complex fading channel coefficient modeling multipath fading has two quadrate components which are zero mean Gaussian random processes. As a result, the amplitude of fading envelope follows a Rayleigh distribution. In terms of error rate performance, Rayleigh fading converts the exponential dependency of the bit-error probability on the signal-to-noise ratio (SNR) for the classical additive white Gaussian noise (AWGN) channel into an approximately inverse linear one, resulting in large SNR penalty.

In order to improve the reliability of transmissions on wireless radio channels, some measures have to be employed in order to reduce the degrading effects of multipath fading. Diversity techniques have been known to be effective in combating the extreme and rapid signal variations associated with the wireless radio transmission path. Diversity improves transmission performance by making use of more than one independently faded version of the transmitted signal. If several replicas of the signals are transmitted over multiple channels that exhibit independent fading with comparable strengths, the probability that all the independently faded signal components experience deep fading simultaneously is significantly reduced. A communication system operating over wireless channels should be designed in a way to exploit as much as diversity as possible. There are several sources that diversity can originate from. The most common methods are briefly summarized below [14], [15].

1.1.1 Frequency Diversity

If the channel behaves frequency-selective [15], its transfer function influences different part of the signal's spectrum diversely. Hence, diversity is obtained in the frequency domain that can be exploited by appropriate receiver structure. For Code division multiple access (CDMA) systems the RAKE receiver [14] exploits frequency diversity by combining different propagation paths being separable in time [16]. In coded Orthogonal Frequency Division Multiplexing (OFDM) systems, the decoding process averages over carriers associated with different channel coefficient [17]. It should be emphasized that frequency diversity can be exploited if the separation between the carriers is at least equal to the coherence bandwidth of the channel [16].

1.1.2 Time Diversity

In this form of diversity, different time slots are used to realize diversity advantage. The message is transmitted repeatedly over several time slots. To ensure independency among multiple diversity channels, the time separation between adjacent transmissions should be larger than the channel coherence time. A sophisticated method to obtain time diversity is channel coding in conjunction with interleaving [17]. This technique is effectively particular for time-selective fading environments. However, it offers little protection under slowly varying fading channels, unless significant interleaving delays can be tolerated.

1.1.3 Space Diversity

Recently, the design of wireless systems using multiple antennas at transmitter and/or receiver side gained much interest. For antenna separations larger than several wavelengths, the channels can be assumed to be independent, so that diversity is obtained even for quasi-static channels where time-diversity cannot be exploited. The required antenna separation depends on the local scattering environment as well as on the carrier frequency. For a mobile station which is near the ground with many scatters around, the channel decorrelates over a shorter distances, and typical antenna separation of half to one carrier wavelength is sufficient. For base stations on high towers, a large antenna separation of several to tens of wavelength may be required [17].

1.1.4 Polarization Diversity

A significant amount of transmitted energy over the radio channel is usually transposed to a polarization state orthogonal to that of the transmitting antenna. This is due to the multipath reflection and scattering that the transmitted signal experiences during its propagation. The use of polarized diversity scheme allows the receiver to take advantage of both co-polarized and cross-polarized states [19]. The main advantage of polarization diversity is that it improves BER performance of the wireless communication systems without requiring the large antenna spacing that is necessary in spatial diversity. The drawback of this technique is that we have to transmit 3 dB more because we have to feed signals to both polarization antennas at the transmitter [18].

1.1.5 Directional Diversity

The received signal at the receiver consists of reflection, diffraction, or scattered signals and they come from incident angles. If we can resolve the received signal by using directive antennas, we can obtain independent faded signals because all of the paths, coming from different angles are mutually independent. When we employ a directive antenna, we can reduce the Doppler spread for each branch [16].

1.1.6 Diversity Combining Methods

After the receiver obtains several replicas of the same signal through diversity channels, it processes them to obtain a single representation of the desired symbol. There are different combining methods depending on the level of channel knowledge at the receiver. Maximum Ratio Combining (MRC) achieves the maximum SNR at the receiver's output by weighting each received replica by the

corresponding complex conjugate channel coefficient and successive summation. Therefore, this method requires the knowledge of amplitude and phase of all involved channels, and requires screening and tracking for all components. In Equal Gain Combining (EGC) the phase rotation for each signal is compensated but the magnitude remains unchanged. This method only requires the phase of all channel coefficients, not the magnitudes. Selection Combining (SC) represents the simplest combining method because it only selects a subset of replicas for further processing and neglects all the remaining signals [22].

1.2 Transmit Diversity

Transmit diversity, a form of spatial diversity, has been studied extensively within the last decade as a powerful method of combating detrimental effects in wireless fading channels [20]-[22]. The deployment of multiple antennas at the base station to facilitate uplink transmission (i.e., receive diversity) has been traditionally used in cellular system. However, the use of multiple antennas at the mobile station is not feasible due to the limitations on size and the expense of multiple down-conversions of RF paths. Despite its obvious advantages, transmit diversity has been viewed as more difficult to exploit in the past, in part because the transmitter is assumed to know less about the channel than the receiver and in part because of the challenging signaling design problem. Within the last decade, transmit diversity has attracted a great deal of attention and practical solutions have been proposed to realize transmit diversity advantages.

Transmit diversity can be classified into two broad categories based on the need for channel state information (CSI) is the transmitter: Close-loop and open-loop schemes. When the transmitter does not have any information about the channel, the system is classified as an “open-loop” system. In this case, the receiver may estimate the channel and uses the CSI for decoding. However, the transmitter does not have access to the CSI. On the contrary, in some systems, the receiver sends some information about the channel back to the transmitter through feedback channel. This is called “close-loop” system and the transmitter can use this information to improve the performance [23]. In the design of close-loop schemes, several other factors such as feedback delay, feedback error, and channel estimation error need to be taken into account.

In open-loop diversity schemes, the receiver estimates and uses the CSI information, but the transmitter does not have the access to CSI. An early example of such schemes has been proposed by Wittenben [24], [25] where the operating frequency-flat channel is converted intentionally into

frequency selective channel to exploit artificial path diversity by means of a maximum likelihood (ML) decoder. The so called "delay diversity" scheme of [24] is optimal in the sense that the diversity advantage experienced by an optimal receiver is equal to the number of transmit antennas [26]. Delay diversity also an ancestor of space-time trellis codes (STTCs) which have been proposed in the 1990's by Tarokh, Seshadri, and Calderbank [27].

1.2.1 Space-time Coding

The information capacity of wireless communication systems can be increased considerably by employing multiple transmit and receive antennas leading to the so-called MIMO (multi-input-multi-output) communications. An effective and practical way to approaching the capacity is to employ space-time coding [27]. Space-time trellis codes (STTCs) combine the channel code design with symbol mapping onto multiple transmit antennas. The data symbols are cleverly coded across space and time to extract diversity advantages. In the pioneering work [27], Tarokh *et al*, have derived the performance criteria for STTCs based on upper bound on pairwise error probability (PEP) for quasi-static and symbol-by-symbol interleaved fading channels. For quasi-static fading channels, error rate performance is shown to be determined by matrices constructed from pair's distinct code sequences. The minimum rank among these matrices qualifies the diversity gain, while minimum determinant quantifies the coding gain. These are known as "rank and determinant" criteria. Whereas, for fast fading channels, space-time code design is governed by "distance and product" criteria, which determines the diversity and coding gain respectively. STTCs provide full diversity, but the complexity of the receiver structure increases exponentially with the number of transmit antenna. Space-time block codes (STBCs) were proposed as an attractive alternative to its trellis counterpart with a much lower decoding complexity. These codes are defined by a mapping operation of a block of input symbols into the space and time domains, transmitting the resulting sequences from different antennas simultaneously. Tarokh et al.'s work in [27] was inspired by Alamouti's early work [20], where a simple two-branch transmit diversity scheme was presented and shown to provide the same diversity order as MRC with two receive antennas. Alamouti's scheme is appealing in terms of its performance and simplicity. It requires a very simple decoding algorithm based only on linear processing at the receiver. STBCs based on orthogonal designs [32] generalizes Alamouti's scheme to an arbitrary number of transmit antennas still preserving the decoding simplicity and are able to achieve the full diversity at full transmission rate for real signal constellations and at half rate for

complex signal constellations such as QAM or PSK. Over the last years several contributions have been made to further improve the data rate of STBCs, e.g., [33], [34] and the references therein.

1.3 Cooperative Diversity

With their significant advantages, MIMO techniques have been already included in various industry standards such as 3rd generation cellular and IEEE 802.11n WLAN standards. Unfortunately, the deployment of multiple antennas might not be practical, if not infeasible, in the uplink of a cellular system, due to the size, power limitations, and hardware complexity of the mobile terminals. Similar restrictions also apply to the wireless sensor networks which are gaining popularity in recent years.

One way to overcome these limitations is cooperative diversity [11]. Cooperative diversity realizes spatial diversity advantages in a distributed manner where a node uses others' antennas to relay its message creating virtual antenna array. The basic idea behind user cooperation can be traced back to Cover and El Gamal's work on the information theoretic properties of the relay channel [30]. The recent surge of interest in cooperative communication was subsequent to the works of Sendonaris et al. [12] and Laneman et al. [11]. In [11], Laneman et al, proposed a user cooperation protocol that is built upon a two-phase transmission scheme. In the first phase (i.e., broadcasting phase), the source broadcast to the destination and relay terminals. In the second phase (i.e., relaying phase), the relay transmits processed version of the received signals to the destination. Source, relay and destination nodes are all equipped with single transmit/receive antennas and operate in *half-duplex* mode (i.e., a node can either transmit or receive at a given time, but cannot do both simultaneously). Cooperative communication requires a user to listen to the transmission from other users and relay this information to the destination. In other words, the users are required to be within the radio range of each other, so that mutual transmissions can be received with reasonable signal strength, at least on an average power.

The user cooperation protocol considered in [11] effectively implements receive diversity in a distributed manner. In [13] Nabar et.al, established a unified framework of cooperation protocols for single-relay wireless networks. They have considered three TDMA-based protocols named Protocol I, Protocol II, and Protocol III, which are briefly described below

- Protocol I: during the first timeslot, the source terminal communicates with the relay and destination. During the second time slot, both the relay and the source terminals

communicate with destination terminal. This protocol realizes the maximum degree of broadcasting and receives collision. Protocol I is referred to as “transmit diversity (TD)” protocol in [35].

- Protocol II: during the first timeslot, the source communicates with the relay and destination terminals. In second time slot only the relay is involved in transmitting the signal to the destination. This is the same cooperation protocol proposed by Laneman et al. in [] and is referred to as “receive diversity (RD) protocol” in [35]
- Protocol III: this is similar to Protocol I, except that the destination terminal does not receive from the source during the first time slot. This protocol does not implement broadcasting but realizes receive collision. This is referred to as “simplified transmit diversity (STD) protocol” in [35]

It can be noticed from the descriptions of protocols that the signal transmitted to both the relay and destination terminals is the same over the two time slots in Protocol II. Therefore, classical space-time code construction does not apply to Protocol II. On the other hand, Protocol I and Protocol III can transmit different signals to the relay and destination terminals. Hence, the conventional STBC can be easily applied to these protocols in a distributed fashion.

The above cooperation protocols can work with various forms of relaying methods. Three popular relay strategies, namely amplify-and-forward (AaF), decode-and-forward (DaF), and amplify/decode-and-forward (ADF) are summarized below

- Amplify-and-forward (AaF): In the amplify-and-forward (AaF) technique, the relay nodes simply scale the received samples to meet the average transmit power constraint and before forwarding to the destination. The key advantages of the AaF technique are that relay nodes do not have to decode the information, reducing the burden on these nodes which would typically be low power mobile devices. However, the disadvantage is that the information symbols, corrupted by inter-user channel distortion, are forwarded along with the receiver noise at the relay node
- Decode and Forward (DaF): A wireless communication system typically takes advantage of digital modulation. In scenarios, where the relay has enough computing power to decode the signal, DaF is preferred. The received signal is first decoded and then re-encoded. So there is no amplified noise in the sent signal, as in the case of AaF. The relay can decode

the original message completely. This requires a lot of computing power, but has the advantage that an error correcting code could be processed at the relay.

- Amplify/decode-and-forward (ADF): In this hybrid version, an ADF relay will use its knowledge of the channel coefficients to make a decision to either act as an AF relay or a decode-and-forward relay. Specifically, if the inter-user channel is not in outage, then each user can perfectly decode the other's information assuming that the transmitted information is encoded using a capacity approaching error control code, and hence forward a clean version to the destination. The ADF relay will decode the received information and forward the decoded symbols to the destination. On the other hand, in the case of an outage, it would be counter-productive to forward erroneously decoded information, so the ADF relay simply amplifies and forwards the packet.

1.4 Research Motivation

Vehicular Communication is entering an exciting phase. Auto-mobile companies are investing huge amount of resources in research to facilitate this technology. In past, most of the work has been directed at routing, security, or Quality of Service (QoS). However, the literature on physical layer modeling and analysis in Vehicular Communications is quite sparse.

In addition to V2V communication, some recent work has addressed the theoretical aspects of cooperative diversity [11] . It has been demonstrated that leveraging on cooperative diversity expands the efficacy of wireless networks by improving the range, the capacity, and the quality. Nevertheless, the available research is not directly applicable to IVC, due to underlying assumption of quasi-static Rayleigh fading channel model. In cellular radio systems, Rayleigh distribution is commonly used to characterize the envelope of a fading signal. The typical assumption is that the wireless communication scenario has a stationary base station antenna above roof-top level and a mobile station at the street level. However, in V2V communication systems, both the transmitter and the receiver are in motion and the elevations of their antennas are relatively lower, invalidating the Rayleigh fading assumption. In order to realize the full potential of cooperative diversity in IVC, an in-depth investigation of performance limits under realistic V2V channel models and enabling techniques to support broadband V2V applications is imperative.

In this research, we try to analyze the performance of our proposed physical layer model over cascaded fading. In addition, we take into account two different types of relay that can be used in

vehicular environments. Since earlier research has demonstrated that significant improvements can be achieved through optimized protocols, we resort to such optimized protocols for analyzing power savings in vehicular environments.

1.5 Outline of the Thesis

The rest of the thesis is organized as follows: in Chapter 2, we introduce the cascaded Rayleigh fading model. We also define the transmission models for access-point assisted and vehicular-assisted communications. In Chapter 3, we derive the PEP expressions for each of the considered model. In Chapter 4, we calculate the union bounds on the BER and present the power allocation methods which are optimum in the sense of minimizing the BER and discus their efficiency for various location of the relay. In Chapter 5, we present a comprehensive Monte-Carlo simulation study to demonstrate BER performance of the IVC, with different type of relays. The performance comparison is done between equal power allocation and optimum power allocation. The conclusion of this thesis is presented in Chapter 6.

Chapter 2
Channel and System Model

The current literature on cooperative diversity is mainly limited to traditional Rayleigh fading channel which is not much realistic for vehicular networks [36]. In this chapter, we first present the theoretical background on "cascaded fading channel" (also known as "double Rayleigh") which has been proposed as a realistic description of wireless fading channels experienced in mobile-to-mobile communications [34]. Later in the chapter, we introduce our cooperative transmission models over cascaded Rayleigh fading channels.

2.1 Cascaded Rayleigh Fading

In cellular systems, base station is stationary, highly elevated and mostly free of scattering, whereas mobile station is at low elevation in a scattering environment. This link model is known as fixed-to-mobile (F-to-M) [38]. The received envelope of F-to-M, under non line-of-sight conditions is Rayleigh fading. In contrast to F-to-M link, both transmitter and the receiver are in motion in vehicular communication. They are equipped with low elevation antenna, causing the local scattering to have an impact on both mobile stations. The statistical properties in F-to-M link therefore differ from those in vehicular communications.

Akki and Haber [39] were the first to develop the statistical model for Mobile-to-Mobile (M-to-M) channels. A propagation model, that can be viewed more realistic in M-to-M communications, is the cascaded (double) Rayleigh model, first indentified by W. Honcharenko et al [40] and V. Erceg et al. [41] in indoor and micro-cellular propagation studies.

Figure 2.1 shows the M-to-M scenario as given in [37]. Where, N is the number of scatters around transmitter and receiver denoted by S_{TN} and R_{TN} respectively. The scattering radii, R_T and R_R are considered large so that the fading processes due to the movement of the mobiles can be considered stationary. The most important assumption in this model is that the distance between the two mobile stations or vehicles should be large enough, so that the scattering around each terminal is determined by two independent groups of scatters [37].

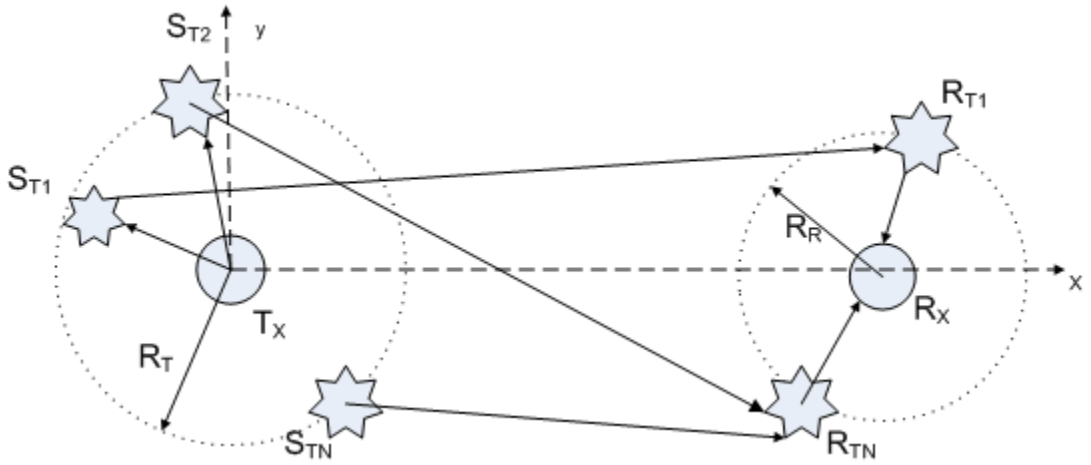

Figure 2.1 Mobile-to-Mobile scattering model

The total signal incident on the n^{th} scattered at the receiver, $s_n(t)$ is the sum of n (complex) signals from the scatters around the transmitter

$$s_n(t) = \sum_{n=1}^{N} A_n \exp\left[j\left(w_{Tn}t + \phi_{Tn}\right)\right] \exp\left(-j\frac{2\pi}{\lambda} d_{TxRx} \right) \tag{2.1}$$

where A_n and ϕ_{Tn} are random variables (reflection/ diffraction coefficients from the scatters), w_{Tn} is the Doppler shift due to the n^{th} transmitter scatters, d_{TxRx} is the distance between the transmitter scatter and the receiver scatter and λ is the wave-length. The total received signal at the receiver $r(t)$ is given by the sum of the contribution from all M scatters around the receiver.

$$\begin{aligned} r(t) = \exp\left(-j\frac{2\pi}{\lambda} d_{TxRx} \right)\left(\sum_{n=1}^{N} A_n \exp\left[j\left(w_{Tn}t + \phi_n + \frac{2\pi}{\lambda}\Delta_n \right)\right]\right) \\ \times\left(\sum_{n=1}^{N} B_m \exp\left[j\left(w_{Rm}t + \phi_m + \frac{2\pi}{\lambda}\Delta_m \right)\right]\right) \end{aligned} \tag{2.2}$$

Using (2.2), we can obtain the narrow-band, time-varying channel transfer function in a 3-D environment

$$H_D(t) = \left(\sum_{n=1}^{N} A_n G_T\left(k_{Tn}\right) \exp\left[j\left(w_{Tn}t + \phi_n\right)\right]\right)\left(\sum_{n=1}^{N} B_m G_R\left(k_{Rn}\right) \exp\left[j\left(w_{Rm}t + \phi_m\right)\right]\right) \tag{2.3}$$

The expression (2.3) derived by I. Z. Kovacs [], presents a very important observation. The channel transfer function obtained here is more general compared to the transfer function obtained in [39]. The signal envelope distribution is given by the product of two independent Rayleigh variables, and

this is the reason for it being called “double Rayleigh” or “cascaded Rayleigh”. This result is different from what J.P.M.G. Linnartz proposed in [42]. Linnartz propagation model assumed the main signal path between two mobile stations to form completely independent paths, without interference at the scatters. Thus, the received signal is given not as a product of independent uniformly distributed random variables. From [43], the distribution of the product of n-independent Rayleigh random variable in terms of Meijer G-Function is given as follows

$$f_Y(y) = 2\left(2^n\sigma^2\right)^{-\frac{1}{2}} G_{0\ n}^{n\ 0}\left(\left(2^n\sigma^2\right)^{-1} y^2 \middle| \begin{matrix} - \\ \frac{1}{2}\cdots\frac{1}{2} \end{matrix}\right) \tag{2.4}$$

where Y is the product of n-Rayleigh random variables, and variance is given by the parameter $\sigma^2 = \Pi_{i=1}^{n}\sigma_i^2$ and Meijer G-Function is a generalization of the hyper-geometric function and is defined using contour integral representation in [44].

Special cases: The equation in (2.4) can be reduced to the case of Rayleigh fading and cascaded Rayleigh fading by assigning n=1 and n=2, respectively. For n=1; we can use the identity defined in [43]

$$G_{0\ 1}^{1\ 0}\left(z\middle|\begin{matrix} - \\ b \end{matrix}\right) = z^b e^{-z} \tag{2.5}$$

By using (2.5), we can obtain the Rayleigh distribution in the following two forms

$$f_Y(y) = 2\left(2\sigma^2\right)^{-\frac{1}{2}} G_{0\ 1}^{1\ 0}\left(\left(2\sigma^2\right)^{-1} y^2 \middle| \begin{matrix} - \\ \frac{1}{2} \end{matrix}\right) \tag{2.6}$$

$$f_Y(y) = \frac{y}{2\sigma^2}\exp\left(\frac{-y^2}{2\sigma^2}\right) \tag{2.7}$$

Similarly for n=2, let us define $z = xy$, where x and y are two independent complex Gaussian random variables, having zero mean and 0.5 variance per dimension. By using the identity as given in [43]

$$G_{0\ 2}^{2\ 0}\left(z\middle|\begin{matrix} - \\ b \end{matrix}\right) = 2z^{\frac{1}{2(b+c)}} K_{b-c}\left(2\sqrt{z}\right) \tag{2.8}$$

The distribution of “double-Rayleigh” can be presented in the following two manners

$$f_Z(z) = \left(\sigma_Z\right)^{-1} G_{0\ 2}^{2\ 0}\left(\left(2^2\sigma_Z{}^2\right)^{-1} z^2 \middle| \begin{matrix} - \\ \frac{1}{2}\cdots\frac{1}{2} \end{matrix}\right) \tag{2.9}$$

$$f_Z(z) = \left(\frac{z}{\sigma_Z{}^2}\right) K_0\left(\frac{z}{\sigma_Z}\right) \tag{2.10}$$

where K_0 is the Zero order modified Bessel function of the second kind [46]. Also $\sigma_Z^2 = \sigma_X^2 \sigma_Y^2$, is the variance of Z. The magnitude $|z|$ follows a cascaded Rayleigh distribution [45].

$$f(|z|) = 4|z| K_0(2|z|) \tag{2.11}$$

With normalized power $E\left[|z|^2\right] = 1$. The detailed derivation of this distribution can also be found in [37].

2.2 Cooperative Transmission Models

We consider a single-relay scenario in which source, relay, and destination nodes operate in half-duplex mode and are equipped with a single pair of transmit and receive antennas. We study two different scenarios based on the relay type

In the first scenario, the relay is considered as road-side infrastructure, which could be an access point or base station depending upon the wireless technology to be implemented by the service provider. The source vehicle is assisted by this relay to send the signal information towards the destination which is also a vehicle. This model is shown in Figure 2.2 and will be referred to as Access Point Assisted (APA) communication. Here h_{SR}, h_{RD}, and h_{SD} represents the fading coefficient of links source-to-relay $(S \to R)$, relay-to-destination $(R \to D)$ and source-to-destination $(S \to D)$ respectively. The channel between source-to-destination $(S \to D)$ is modeled as cascaded Rayleigh fading channels. Therefore, h_{SD} is assumed to be product of two i.i.d (independent and identically distributed) complex Gaussian random variables each of which has zero mean and variance of 0.5 per dimension. The fading model for the other two links, source-to-relay $(S \to R)$ and relay-to-destination $(R \to D)$ is considered as Rayleigh. Therefore, h_{SR} and h_{RD} are assumed to be i.i.d zero mean complex Gaussian random variables with variance 0.5 per dimension. Rayleigh fading assumption in these links is justified considering that the relay node is an AP elevated above the street level.

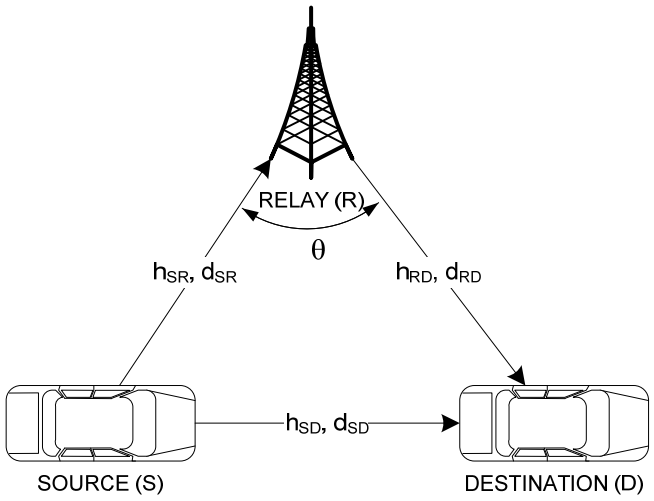

Figure 2.2 Access point assisted Communication (APA)

In the second scenario, all the three nodes are considered as vehicles and underlying links are modeled as cascaded Rayleigh. This scenario is depicted in Figure 2.3 and will be referred to as Vehicular Assisted (VA) communications. In vehicle-assisted scenario, all underlying links are modeled as cascaded Rayleigh. Therefore h_{SD}, h_{RD} and h_{SR} are assumed to be products of i.i.d complex Gaussian random variables each of which has zero mean and variance of 0.5 per dimension.

In both models the parameters $(d_{SD}, d_{SR}$ and $d_{RD})$ are the distances between $S \to D$, $S \to R$ and $R \to D$ respectively, and θ is the angle between $S \to R$, and $R \to D$.

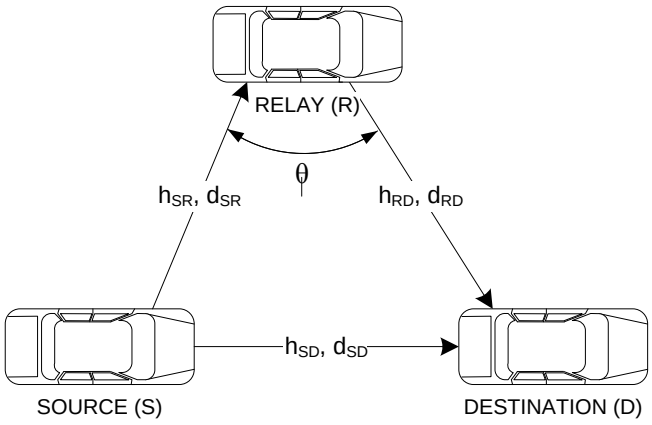

Figure 2.3 Vehicular Assisted Communications (VA)

2.3 Path loss Model

We assume an aggregate channel model which takes into account both long-term path loss and short-term fading. This lets us to explicitly consider the effects of relay location in our transmission model. The path loss between any two nodes A and B can be modeled by

$$Loss(A,B) = \frac{D}{d_{AB}^{\alpha}} \tag{2.12}$$

where D is a constant that depends on the propagation environment, d_{AB} is the Euclidean distance between nodes A and B, and α is the path loss coefficient. Typical values of α can be found in Table 2.1 for various wireless channel environments

Table 2.1 Path loss coefficient in different environments [1]

Environment	Path loss exponent
Free Space	2
Urban Area Cellular Radio	2.7-3.7
Shadowed Urban Area Cellular Radio	3-5
In building Line of Sight	1.6-1.8

Assuming the path loss between $S \to D$ to be unity, the relative geometrical gain of $S \to R$ and $R \to D$ links are defined, respectively,

$$G_{SR} = \frac{Loss(S,R)}{Loss(S,D)} = \left(\frac{d_{SD}}{d_{SR}}\right)^2 \tag{2.13}$$

$$G_{RD} = \frac{Loss(R,D)}{Loss(S,D)} = \left(\frac{d_{SD}}{d_{RD}}\right)^2 \tag{2.14}$$

This can further be related to each other by the Pythagorean Theorem as,

$$G_{RD} + G_{SR} - 2\sqrt{G_{RD}G_{SR}}\cos\theta = G_{RD}G_{SR} \tag{2.15}$$

We further define the relative geometrical gain as

$$\beta = \frac{G_{SR}}{G_{RD}} = \left(\frac{d_{RD}}{d_{SR}}\right)^2 \tag{2.16}$$

The relay location will be indicated by β. The more negative the ratio (given in dB), the closer is the relay located to the destination. On the other hand, positive values indicate the relay and source

are closer. The particular case of the β = 0dB means that both source and destination terminals have same distance to the relay. In terms of β, we can further rewrite G_{SR} and G_{RD} as

$$G_{SR} = 1 + \beta - 2\sqrt{\beta}\cos\theta \tag{2.17}$$

$$G_{RD} = \frac{1 + \beta - 2\sqrt{\beta}\cos\theta}{\beta} \tag{2.18}$$

2.4 Signal Model

Our signal model is based on Protocol II for user cooperation. This method effectively implements a single-input-multiple-output (SIMO). Let x denote the transmitted signal in the first time slot. We assume M-PSK (phase shift keying) modulation with normalized unit energy for the signals, i.e., $E[|x|^2] = 1$. Considering path-loss effect, the received signal at the relay and destination are given as

$$r_R = \sqrt{2G_{SR}\Lambda E}\,h_{SR}x + n_R \tag{2.19}$$

$$r_{D1} = \sqrt{2\Lambda E}\,h_{SD}x + n_{D1} \tag{2.20}$$

where the total energy (to be used by both source and relay terminals) is 2E during two timeslots yielding an average power in proportion to E per time slot, Λ is the optimization parameter which controls the fraction of power reserved for the broadcasting phase. For equal power allocation the value for Λ is assigned to be 0.5. n_R, and n_{D1}, are the independent samples of a zero-mean complex Gaussian random variable with variance $N_0/2$ per dimension, which models the additive noise term. Here h_{SR} and h_{SD}, represents the fading coefficients for $S \to R$ and $S \to D$ links respectively.

The relay terminal normalizes the received signal r_R by a factor of $\sqrt{E\left[\left|r_R\right|^2\right]}$ to ensure the unity of average of energy and re-transmits the signal during the second time slot. Therefore, the received signal at the destination terminal in the second time slot is given as

$$r = \sqrt{2G_{RD}\left(1-\Lambda\right)E}\,h_{RD}\frac{r_R}{\sqrt{E[|r_R|^2]}}x + \tilde{n} \tag{2.21}$$

where, $\tilde{n}$ is the additive noise term modeled as a zero-mean complex Gaussian random variable with variance $N_0/2$ per dimension. The normalization factor is calculated as

$$E\left[\left|r_R\right|^2\right] = 2G_{SR}\Lambda E + N_0 \tag{2.22}$$

Substituting (2.22) into (2.21), we obtain

$$r = 2E\sqrt{\frac{G_{SR}G_{RD}(1-\Lambda)}{2G_{SR}\Lambda E + N_0}}h_{RD}h_{SR}x + \tilde{n} \tag{2.23}$$

where, the effective noise term $\tilde{n}$ is defined as

$$\tilde{n} = \sqrt{\frac{2G_{RD}(1-\Lambda)E}{2G_{SR}\Lambda E + N_0}}h_{RD}n_R + \tilde{n}_{D2} \tag{2.24}$$

conditioned on h_{RD}, $\tilde{n}_{D2}$ is found out to be Gaussian with zero mean and variance of

$$E\left[\left|\tilde{n}\right|^2 \left|h_{RD}\right.\right] = \left(1 + \frac{2G_{RD}(1-\Lambda)E\left|h_{RD}\right|^2}{2G_{SR}\Lambda E + N_0}\right)N_0 \tag{2.25}$$

We assume that the destination terminal normalizes the received signal given by (2.19)

$$\text{with}\sqrt{\frac{1+2G_{RD}(1-\Lambda)E\left|h_{RD}\right|^2}{(2G_{SR}\Lambda E + N_0)}} \tag{2.26}$$

resulting in,

$$r'_{D2} = \sqrt{\gamma}\sqrt{E}h_{SD}h_{RD}x + n'_{D2} \tag{2.27}$$

where,

$$\gamma_1 = \frac{2G_{SR}\Lambda}{\left|h_{RD}\right|^2 + A_1} \tag{2.28}$$

$$A_1 = \frac{2G_{SR}\Lambda SNR + 1}{2G_{RD}(1-\Lambda)SNR} \tag{2.29}$$

Equation (2.20) and (2.27) can be written in a matrix form of

$$\mathbf{r} = \mathbf{hX} + \mathbf{n} \tag{2.30}$$

where,

$$\mathbf{h} = \begin{bmatrix} h_{SD} & h_{SR}h_{RD} \end{bmatrix} \tag{2.31}$$

and,

$$\mathbf{X} = \begin{bmatrix} \sqrt{2\Lambda}\sqrt{E}x & 0 \\ 0 & \sqrt{\gamma_1}\sqrt{E}x \end{bmatrix} \tag{2.32}$$

Chapter 3
Diversity Gain Analysis

In this chapter, we investigate the achievable diversity orders for cooperative vehicular scenarios under consideration through the derivation of the pairwise error probability (PEP). PEP is the building block for the derivation of union bound to the error probability and is commonly used for diversity gain analysis where closed-form error rate expressions are unavailable.

Let $\mathbf{X}$ denote the transmitted codeword and assume the receiver makes a decoding error and chooses another codeword $\widehat{\mathrm{X}}$. PEP is the probability of choosing $\hat{\mathbf{X}}$ instead of $\mathbf{X}$ and is denoted by $P\left(\mathbf{X}\to\hat{\mathbf{X}}\right)$. The conditional PEP given fading coefficient can be written as

$$P\left(\mathbf{X}\to\hat{\mathbf{X}}\middle|\mathbf{h}\right)=Q\left(\sqrt{\frac{d^2\left(\mathbf{X},\hat{\mathbf{X}}\right)}{2N_0}}\right) \tag{3.1}$$

where $Q(\bullet)$ is the Gaussian Q-function defined by [16] and $d^2\left(\mathbf{X},\hat{\mathbf{X}}\right)$ denotes the Euclidean distance between $\mathbf{X}$ and $\hat{\mathbf{X}}$ and is given by

$$d^2\left(\mathbf{X},\hat{\mathbf{X}}\right)=\mathbf{h}\left(\mathbf{X}-\hat{\mathbf{X}}\right)\left(\mathbf{X}-\hat{\mathbf{X}}\right)^H\mathbf{h}^H \tag{3.2}$$

Using the Chernoff bound on Gaussian Q-function, an upper bound on PEP is given by [47]

$$P\left(\mathbf{X}\to\hat{\mathbf{X}}\middle|\mathbf{h}\right)\le\exp\left(-\frac{d^2\left(\mathbf{X},\hat{\mathbf{X}}\right)}{4N_0}\right) \tag{3.3}$$

Using (3.2), we obtained the following

$$d^2\left(\mathbf{X},\hat{\mathbf{X}}\right)=2\Lambda E\chi\left|h_{SD}\right|^2+\gamma_1 E\chi\left|h_{SR}\right|^2\left|h_{RD}\right|^2 \tag{3.4}$$

where $\chi=\left|x-\hat{x}\right|^2$. Now substituting (3.4) in (3.3)

$$P\left(\mathbf{X}\to\hat{\mathbf{X}}\middle|h_{SD},h_{SR},h_{RD}\right)\le\exp\left(\left(-\frac{SNR\chi}{4}\right)\left(2\Lambda\left|h_{SD}\right|^2+\gamma_1\left|h_{SR}\right|^2\left|h_{RD}\right|^2\right)\right) \tag{3.5}$$

3.1 PEP for APA Cooperative Scheme

Recall that the link $S\to D$ is modeled as cascaded faded. Define $\left|h_{SD}\right|^2=\left|\alpha\right|^2\left|\beta\right|^2$, where $\left|\alpha\right|^2$ and $\left|\beta\right|^2$ are two independent complex Gaussian random variables, having zero mean and 0.5 variance per dimension, and they follow exponential distribution, (3.5) can be re-written as

$$P\left(\mathbf{X}\to\hat{\mathbf{X}}\left|\alpha,\beta,h_{SR},h_{RD}\right.\right)\le\exp\left(\left(-\frac{SNR\chi}{4}\right)\left(2\Lambda\left|\alpha\right|^2\left|\beta\right|^2+\gamma_1\left|h_{SR}\right|^2\left|h_{RD}\right|^2\right)\right) \tag{3.6}$$

now, averaging over $\left|\alpha\right|^2$

$$P\left(\mathbf{X}\to\hat{\mathbf{X}}\left|\beta,h_{SR},h_{RD}\right.\right)\le\left(\frac{2\Lambda SNR\chi}{4}\left|\beta\right|^2\right)^{-1}\exp\left(-\frac{SNR\chi}{4}\left(\gamma_1\left|h_{SR}\right|^2\left|h_{RD}\right|^2\right)\right) \tag{3.7}$$

following through, we average (3.6) with respect to $\left|\beta\right|^2$

$$\begin{aligned}P\left(\mathbf{X}\to\hat{\mathbf{X}}\left|h_{SR},h_{RD}\right.\right)\le&\left(\frac{2\Lambda SNR\chi}{4}\right)^{-1}\exp\left(\left(\frac{2\Lambda SNR\chi}{4}\right)^{-1}\right)\Gamma\left(0,\left(\frac{2\Lambda SNR\chi}{4}\right)^{-1}\right)\\&\times\exp\left(-\frac{SNR\chi}{4}\left(\gamma_1\left|h_{SR}\right|^2\left|h_{RD}\right|^2\right)\right)\end{aligned} \tag{3.8}$$

Where $\Gamma\left(.,.\right)$ is the incomplete Gamma function [48]. After taking the expectation over $\left|h_{SD}\right|^2$, we consider the links $S\to R$ and $R\to D$, which Rayleigh fading links are. Taking the expectation over $\left|h_{SR}\right|^2$ and $\left|h_{RD}\right|^2$

$$\begin{aligned}P\left(\mathbf{X}\to\hat{\mathbf{X}}\left|h_{RD}\right.\right)\le&\left(\frac{2\Lambda SNR\chi}{4}\right)^{-1}\exp\left(\left(\frac{2\Lambda SNR\chi}{4}\right)^{-1}\right)\Gamma\left(0,\left(\frac{2\Lambda SNR\chi}{4}\right)^{-1}\right)\\&\times\left(1+\frac{\gamma_1 SNR\chi}{4}\left|h_{RD}\right|^2\right)^{-1}\end{aligned} \tag{3.9}$$

substituting for γ_1

$$\begin{aligned}P\left(\mathbf{X}\to\hat{\mathbf{X}}\left|h_{RD}\right.\right)\le&\left(\frac{2\Lambda SNR\chi}{4}\right)^{-1}\exp\left(\left(\frac{2\Lambda SNR\chi}{4}\right)^{-1}\right)\Gamma\left(0,\left(\frac{2\Lambda SNR\chi}{4}\right)^{-1}\right)\\&\times\left(1+\frac{2G_{SR}\Lambda SNR\chi}{4\left(\left|h_{RD}\right|^2+A_1\right)}\left|h_{RD}\right|^2\right)^{-1}\end{aligned} \tag{3.10}$$

After performing some basic manipulations

$$\begin{aligned}P\left(\mathbf{X}\to\hat{\mathbf{X}}\left|h_{RD}\right.\right)\le&\left(\frac{2\Lambda SNR\chi}{4}\right)^{-1}\exp\left(\left(\frac{2\Lambda SNR\chi}{4}\right)^{-1}\right)\Gamma\left(0,\left(\frac{2\Lambda SNR\chi}{4}\right)^{-1}\right)\\&\times\left(\frac{A_1+\left|h_{RD}\right|^2}{A_1+\left(1+2G_{SR}\Lambda SNR\chi\right)\left|h_{RD}\right|^2}\right)\end{aligned} \tag{3.11}$$

Using the divide operation to get $\left|h_{RD}\right|^2$ only in the denominator

$$P\left(\mathbf{X}\to\hat{\mathbf{X}}\middle|h_{RD}\right)\le\left(\frac{2\Lambda SNR\chi}{4}\right)^{-1}\exp\left(\left(\frac{2\Lambda SNR\chi}{4}\right)^{-1}\right)\Gamma\left(0,\left(\frac{2\Lambda SNR\chi}{4}\right)^{-1}\right)$$
$$\times\left(1+\frac{G_{SR}\Lambda SNR\chi}{2}\right)^{-1}\left(\frac{A_1-\dfrac{A_1}{1+\dfrac{G_{SR}\Lambda SNR\chi}{2}}}{\dfrac{A_1}{1+\dfrac{G_{SR}\Lambda SNR\chi}{2}}+\left|h_{RD}\right|^2}\right) \tag{3.12}$$

Now averaging over $\left|h_{RD}\right|^2$, this follows exponential distribution. Therefore, we obtain

$$P\left(\mathbf{X}\to\hat{\mathbf{X}}\middle|h_{RD}\right)\le\left(\frac{2\Lambda SNR\chi}{4}\right)^{-1}\exp\left(\left(\frac{2\Lambda SNR\chi}{4}\right)^{-1}\right)\Gamma\left(0,\left(\frac{2\Lambda SNR\chi}{4}\right)^{-1}\right)\left(1+\frac{G_{SR}\Lambda SNR\chi}{2}\right)^{-1}$$
$$\times\left(A_1-\frac{A_1}{1+\dfrac{G_{SR}\Lambda SNR\chi}{2}}\right)\int_0^{\infty}\left(\frac{1}{\left|h_{RD}\right|^2+\dfrac{A_1}{1+\dfrac{G_{SR}\Lambda SNR\chi}{2}}}\right)\exp\left(-\left|h_{RD}\right|^2\right)d\left|h_{RD}\right|^2 \tag{3.13}$$

Eq. (3.13) has a similar form of [48, pp.366, 3.384] and readily yields a closed-form solution. The final unconditional PEP expression for APA can be given as

$$P\left(\mathbf{X}\to\hat{\mathbf{X}}\right)\le\left(\frac{\Lambda SNR\chi}{2}\right)^{-1}\left[\exp\left(\frac{\Lambda SNR\chi}{2}\right)^{-1}\Gamma\left(0,\left(\frac{\Lambda SNR\chi}{2}\right)^{-1}\right)\right]\left(1+\frac{G_{SR}\Lambda SNR\chi}{2}\right)^{-1}$$
$$\times\left[1+A_1\left(1-\left(1+\frac{G_{SR}\Lambda SNR\chi}{2}\right)^{-1}\right)\exp\left(A_1\left(1+\frac{G_{SR}\Lambda SNR\chi}{2}\right)^{-1}\right)\right. \tag{3.14}$$
$$\left.\times\Gamma\left(0,A_1\left(1+\frac{G_{SR}\Lambda SNR\chi}{2}\right)^{-1}\right)\right]$$

In Figure 3.1we compare the derived PEP expression with the exact one. It is observed that our PEP expression matches exactly to the "exact" Chernoff bound given by (3.3). Assuming equal power allocation (i.e., $\Lambda=0.5$), equal distances among all nodes ($G_{SR}=1, G_{RD}=1, G_{SD}=1$), and sufficiently high SNR, (3.14) reduces to

$$P(X,\hat{X})\le 4\left(\chi SNR\Lambda\right)^{-2}\left(1+\frac{\Lambda}{1-\Lambda}\right) \tag{3.15}$$

which illustrates the diversity order of two is available.

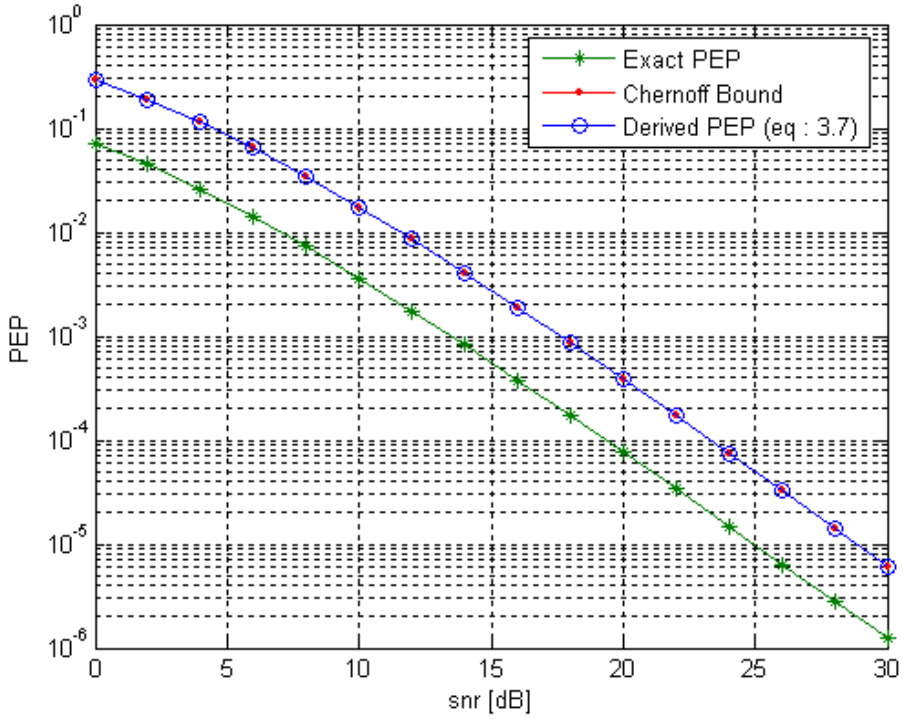

Figure 3.1 Comparison of exact PEP, Chernoff bound and derived PEP at β = -30dB

In order to understand the diversity gain analysis, we have plot the effective (instantaneous) diversity order [45] which is simply the slope of derived as a function of average SNR on a log-log scale, i.e., $\log P\left(\mathbf{X}, \hat{\mathbf{X}}\right) / \log SNR$. In Figure 3.2, we have included as a bench mark the performance of the maximum ratio combining (MRC) with two co-located antennas in conventional Rayleigh fading channel. Another benchmark is single–relay AF system with the same cooperative protocol (protocol II), but over a conventional Rayleigh fading. It can be seen from the figure that performance over the Rayleigh fading converges to its asymptomatic value of two very fast. Whereas, the convergence is affected due to the cascaded nature of the environment and it is relatively slow in approaching asymptomatic value of two.

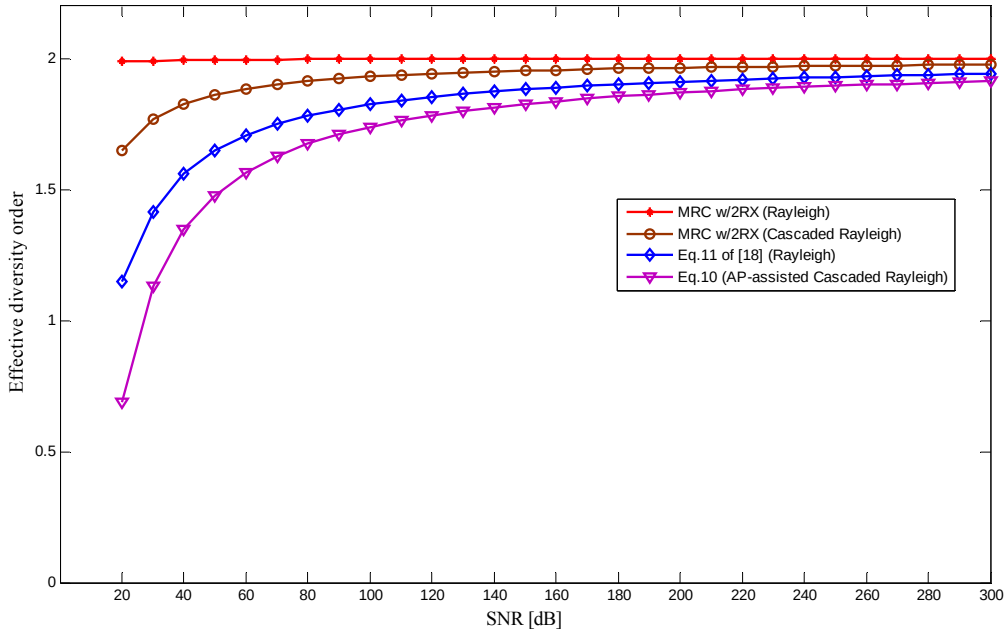

Figure 3.2 Effective diversity order for APA system over conventional and cascaded Rayleigh fading.

3.2 PEP (Vehicular Assisted)

The underlying assumption in this model is that all links $S \to D$, $S \to R$ and $R \to D$ are influenced by cascaded Rayleigh fading. In previous section, we already obtained the PEP expression average over the cascaded link $S \to D$ in (3.14). We can model the fading coefficients of the remaining two links as $|h_{SR}| = |\alpha_1||\beta_1|$, and, $|h_{RD}| = |\alpha_2||\beta_2|$. We re-write (3.7) as

$$P\left(\mathbf{X} \to \hat{\mathbf{X}} \middle| \alpha_1, \beta_1, \alpha_2, \beta_2\right) \le \left(\frac{2\Lambda SNR\chi}{4}\right)^{-1} \exp\left(\left(\frac{2\Lambda SNR\chi}{4}\right)^{-1}\right) \Gamma\left(0, \left(\frac{2\Lambda SNR\chi}{4}\right)^{-1}\right) \times \exp\left(-\frac{SNR\chi}{4}\left(\gamma_1 |\alpha_1|^2 |\beta_1|^2 |\alpha_2|^2 |\beta_2|^2\right)\right) \tag{3.16}$$

Recall that the distribution for the product of two independent Rayleigh random variables is given as (e.g. $|z| = |x||y|$)

$$f_Z(z) = (\sigma_z)^{-1} G_{0\ 2}^{2\ 0}\left(\left(2^2 \sigma_Z{}^2\right)^{-1} z^2 \middle|_{\frac{1}{2}, \frac{1}{2}}^{-}\right) \tag{3.17}$$

Let $k = |z|^2 = |x|^2 |y|^2$, in order to find the distribution of k, we use the following transformation [49]

$$p_K(k) = f_Z(z)\left|g'(z)\right|^{-1} \tag{3.18}$$

where $g'(z)$ is the derivative of g(z). Substituting for $f_Z(z)$ and $g'(z)$, we obtain the distribution of k

$$f_K(k) = \frac{1}{2\sigma_k\sqrt{k}} G_{0\ 2}^{2\ 0}\left(\left(4\sigma_k{}^2\right)^{-1} k \left| \begin{matrix} - \\ \frac{1}{2},\frac{1}{2} \end{matrix} \right.\right) \tag{3.19}$$

Let us now define $y_1 = \left|h_{SR}\right|^2 = \left|\alpha_1\right|^2\left|\beta_1\right|^2$ and $y_2 = \left|h_{RD}\right|^2 = \left|\alpha_2\right|^2\left|\beta_2\right|^2$. By using the above derived distribution, averaging (3.16) with respect to y_1 and using [48, Eq. 7.8131.1], we obtain

$$\begin{aligned} P\left(\mathbf{X}\to\hat{\mathbf{X}}\middle|y_2\right) \le & \left(\frac{2\Lambda SNR\chi}{4}\right)^{-1} \exp\left(\left(\frac{2\Lambda SNR\chi}{4}\right)^{-1}\right)\Gamma\left(0,\left(\frac{2\Lambda SNR\chi}{4}\right)^{-1}\right) \\ & \times \frac{1}{2\sigma_{y1}}\left(\frac{\gamma_1\chi SNRy_2}{4}\right)^{\frac{-1}{2}} G_{1\ 2}^{2\ 1}\left(\frac{\left(\sigma_y{}^2\right)^{-1}}{\gamma_1\chi SNRy_2}\left| \begin{matrix} \frac{1}{2},- \\ \frac{1}{2},\frac{1}{2} \end{matrix} \right.\right) \end{aligned} \tag{3.20}$$

Now taking the expectation over y_2 to obtain the unconditional PEP for VA

$$\begin{aligned} P\left(\mathbf{X}\to\hat{\mathbf{X}}\right) \le & \left(\frac{2\Lambda SNR\chi}{4}\right)^{-1} \exp\left(\left(\frac{2\Lambda SNR\chi}{4}\right)^{-1}\right)\Gamma\left(0,\left(\frac{2\Lambda SNR\chi}{4}\right)^{-1}\right) \\ & \times \frac{1}{4\sigma_{y1}\sigma_{y2}}\left(\frac{G_{SR}\gamma\chi SNR\Lambda}{2}\right)^{\frac{-1}{2}} \int_0^\infty \frac{\sqrt{A_1+y_2}}{y_2} G_{1\ 2}^{2\ 1}\left(\frac{\left(\sigma_y{}^2\right)^{-1}}{(G_{SR}\chi SNR\Lambda)}\left(1+\frac{A_1}{y_2}\right)\left| \begin{matrix} \frac{1}{2},- \\ \frac{1}{2},\frac{1}{2} \end{matrix} \right.\right) \\ & \times G_{0\ 2}^{2\ 0}\left(\left(4\sigma_y{}^2\right)^{-1} y_2 \left| \begin{matrix} - \\ \frac{1}{2},\frac{1}{2} \end{matrix} \right.\right) d\left|y_2\right|^2 \end{aligned} \tag{3.21}$$

Unfortunately, a closed-form solution for (3.21) is not available. This single integration can be evaluated through commercially available mathematics software. In software's, where Meijer G-Function is not defined it can be transformed into Bessel function [46] if necessary.

In Figure 3.3, we compare our PEP expression (3.21) with exact PEP and Chernoff bound. Furthermore we provide the effective diversity order, similar to APA. In Figure 3.4, we plot the effective diversity order for vehicle-assisted relay scenario under consideration. It is observed that the convergence is slower than that of AP-assisted scenario due to the additional degradation resulting from cascaded Rayleigh channels in $S \to R$ and $R \to D$ links.

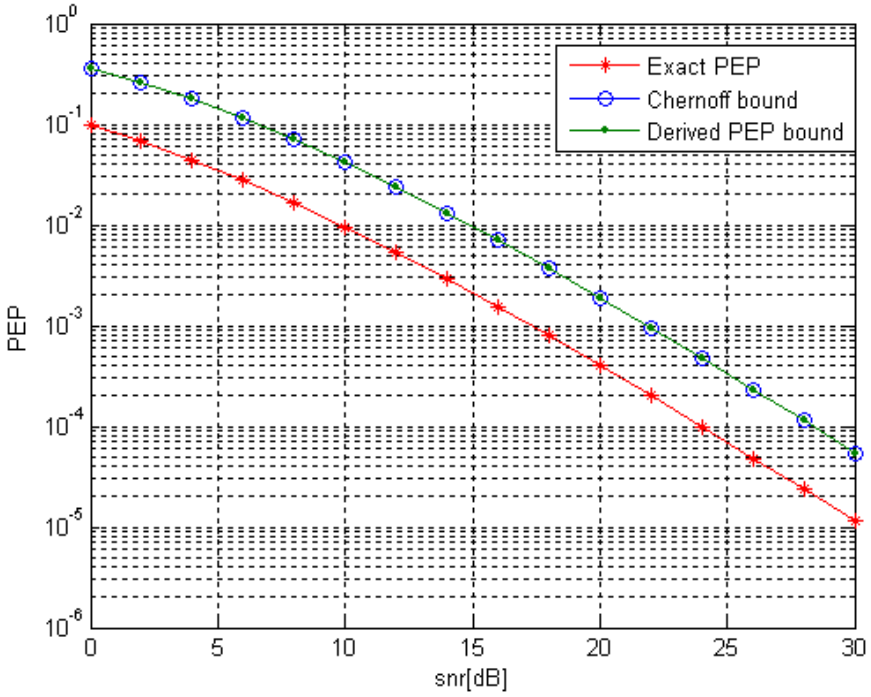

Figure 3.3 Comparison of exact PEP, Chernoff bound and Derived PEP at β =-30dB

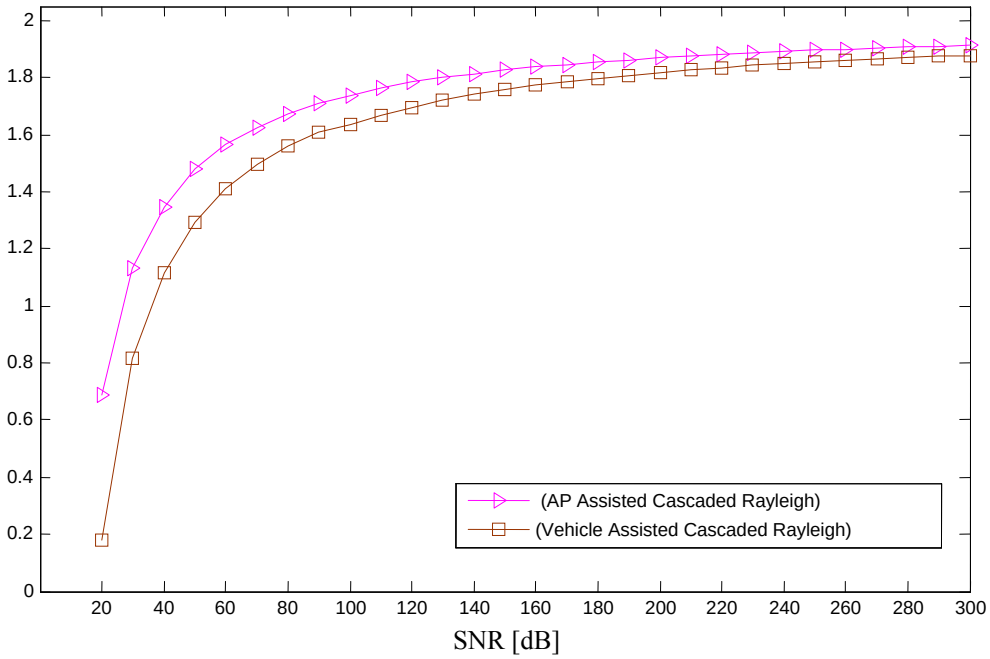

Figure 3.4 Effective diversity order for APA and VP models

Chapter 4

OPTIMUM POWER ALLOCATION

Optimum power allocation (OPA) is a key technique to realize the full potentials of relay-assisted transmission promised by the recent information-theoretic results. The performance of cooperative communication can be significantly improved by the optimal distribution of power between the participating nodes as shown in many recent works [51]-[53]. In this chapter, we determine the optimum power allocation procedures for APA and VA cooperative schemes under consideration. We first derive a union bound on the BER which will be later used as an objective function for the optimization of power allocation

4.1 Union Bound on BER Performance

We consider BER performance as our objective function for power allocation problem under consideration. A union bound on the BER for coded systems is given by [51]

$$P_b \le \frac{1}{n}\sum_{\mathbf{X}} p(\mathbf{X}) \sum_{\mathbf{X}\neq\hat{\mathbf{X}}} q\left(\mathbf{X}\to\hat{\mathbf{X}}\right) P\left(\mathbf{X}\to\hat{\mathbf{X}}\right) \tag{4.1}$$

Where, $p(\mathbf{X})$ is the probability that codeword $\mathbf{X}$ is transmitted, $q\left(\mathbf{X}\to\hat{\mathbf{X}}\right)$ is the number of information bits errors in choosing another codeword $\hat{\mathbf{X}}$, instead of the original one. The variable *n* is the number of information bits per transmission, and $p\left(\mathbf{X}\to\hat{\mathbf{X}}\right)$ denotes the PEP. The required PEP expressions for this calculation have been already obtained in the previous chapter. PEPs for APA and VA schemes are given by (3.14) and (3.21), respectively.

The specific form of BER expressions depend on the modulation scheme. In the following, the union bounds for BPSK, 4-PSK, 8-PSK, 16-PSK and 16-QAM are provided. Let χ be the Euclidean distance between any two signals in the constellation and assume $f(\chi) \triangleq P(\mathbf{X}\to\hat{\mathbf{X}})$

$$P_{b,BPSK} \le f(\chi=4) \tag{4.2}$$

$$P_{b,QPSK} \le f(\chi=4)+f(\chi=2) \tag{4.3}$$

$$P_{b,8-PSK} \le f(\chi=2)+1.5f(\chi=3.41)+0.33f(\chi=4)+1.67f(\chi=0.58) \tag{4.4}$$

$$\begin{aligned} P_{b,16-PSK} \le\ & 0.5f(\chi=4)+1.25f(\chi=3.847)+1.5f(\chi=3.412)+1.25f(\chi=2.765) \\ & +f(\chi=2)+f(\chi=1.234)+f(\chi=0.5858)+0.5f(\chi=0.152) \end{aligned} \tag{4.5}$$

$$P_{b,16-QAM} \le 0.75 f(\chi = 5.2) + 0.125 f(\chi = 7.2) + 0.75 f(\chi = 4) + 2.25 f(\chi = 2) + f(\chi = 3.2) + 1.12 f(\chi = 0.8) + 0.25 f(\chi = 3.6) + 0.75 f(\chi = 0.4) + f(\chi = 1.6) \quad (4.6)$$

In Figure 4.1 and Figure 4.2, we provide comparisons between the union bounds associated with the exact PEP and derived upper bound at relay location β = -30dB for APA and VA schemes assuming BPSK

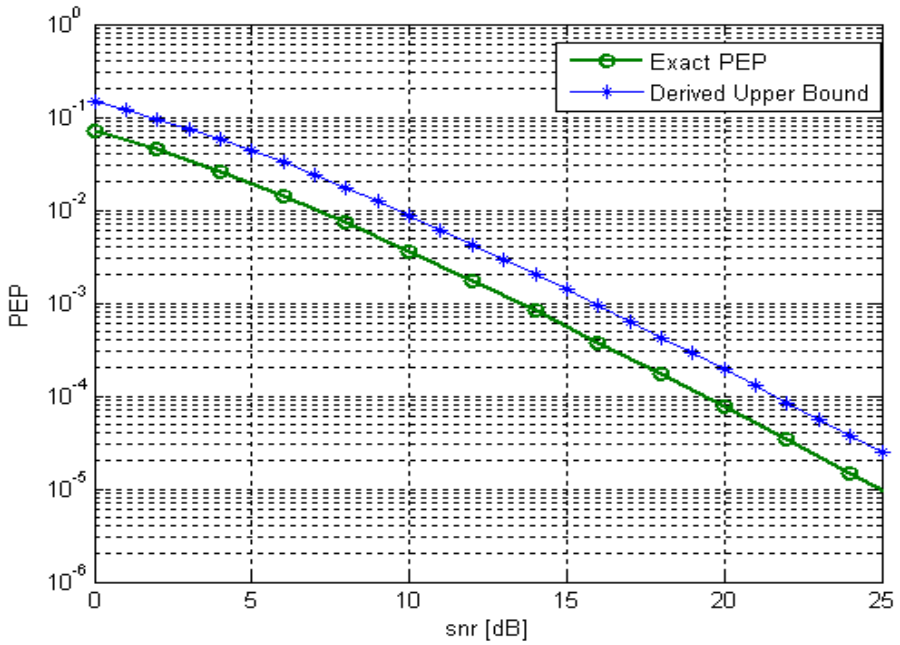

Figure 4.1 Comparison of union bound on exact PEP and derived upper bound for APA

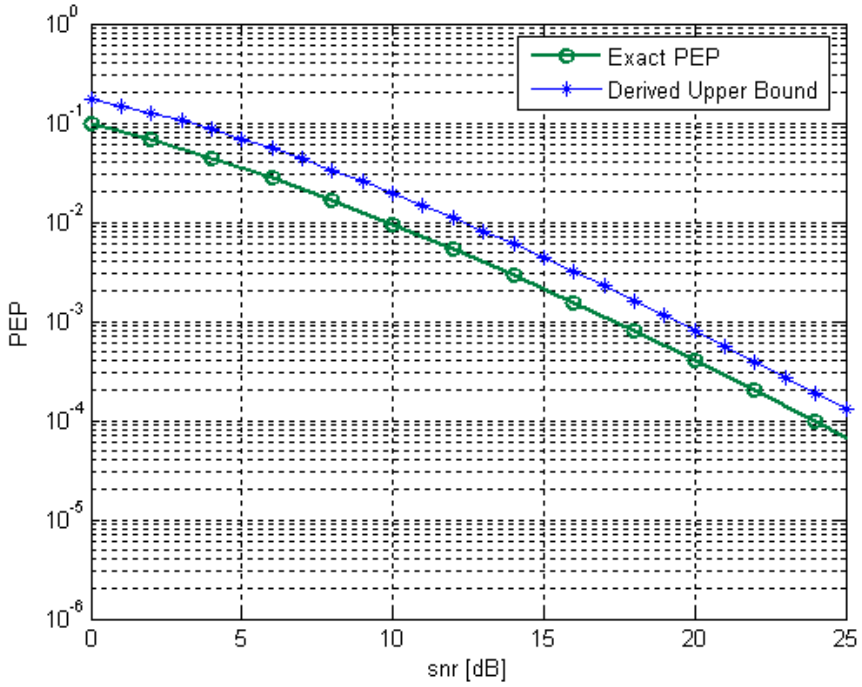

Figure 4.2 Comparison of union bound on exact PEP and derived upper bound for VA

4.2 Optimum Power Allocation Method

As mentioned in the previous section the optimal power allocation rule is based on the minimization of a union bound on the bit error rate (BER) performance. The power allocation parameter in our model is represented as Λ. The value range is given as $0 \le \Lambda \le 1$. It can be readily checked that the union bounds on BER are convex functions with respect to Λ. See for example Figure 4.3 and Figure 4.4, where we plot (4.3) with respect to Λ for various values of SNR under AP-assisted and Vehicular-assisted scenarios, respectively. The objective function is found to be convex with respect to optimization parameter Λ. Convexity of the function under consideration guarantees that local minimum found through optimization will indeed be a global minimum.

The analytical solution is unfortunately is very difficult, if not infeasible. To overcome this limitation we have used MATLAB toolbox "fimincon" to find the minimum of our objective function with respect to Λ. This command is designed to find the minimum of constrained nonlinear multivariable function. It implements a sequential quadratic programming (SQP) algorithm. At each, iteration of the algorithm, an approximation of the Hessian of the Lagrangian function is calculated

using a quasi-Newton updating method. This is then used to generate a quadratic programming sub-problem whose solution is used to form a search direction for a line search procedure

It should be emphasized that for practical systems this problem need not be solved in real-time, because optimization does not depend on the instantaneous channel information or the input data. This mean that the OPA values can be obtained apriori for given values of operating SNR and propagation parameters, and can be used as a lookup table in practical implementation

.

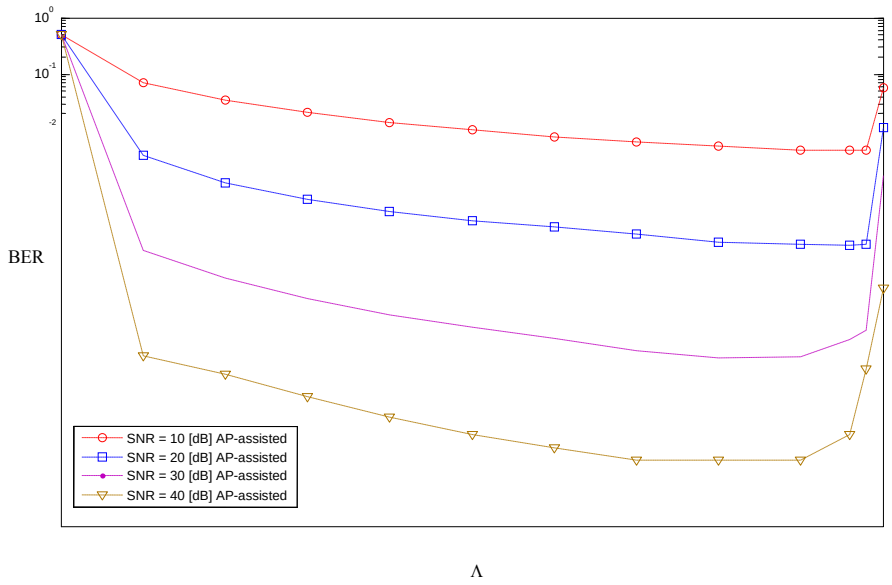

Figure 4.3 BER versus Λ ($\beta = -30$ dB, 4-PSK, $\theta = \pi$, and $\alpha = 2$).

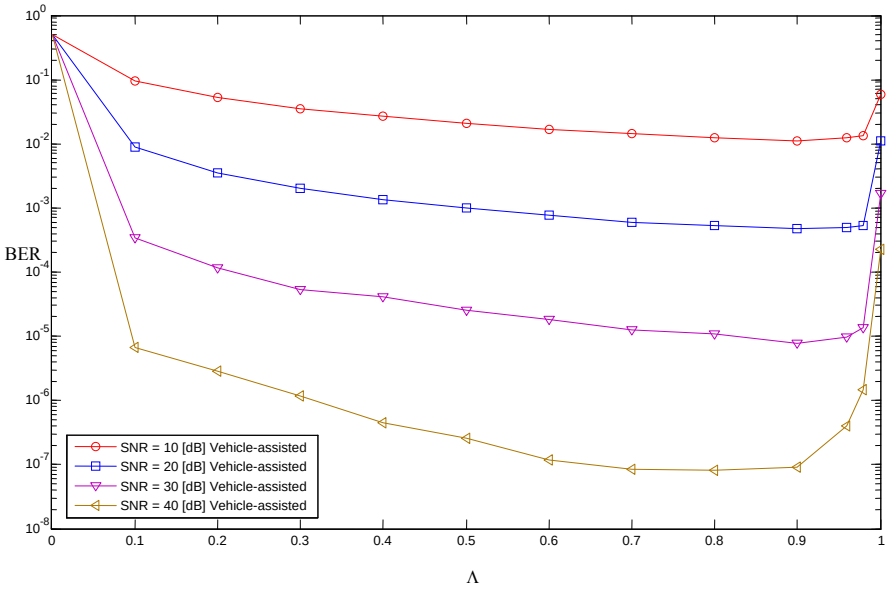

Figure 4.4 BER versus Λ ($\beta = -30$ dB, 4-PSK, $\theta = \pi$, and $\alpha = 2$).

4.2.1 Power Allocation (APA)

In Tables (4.1- 4.4), we present the optimum power allocation values for APA. We have assumed $\theta = \pi$, and path loss coefficient $\alpha = 2$ for different modulation schemes. For the purpose of clearly identifying the change trend of optimum values, we have considered three distinct relay locations. The relay locations are identified as, close to destination $\beta = -30dB$, equal distances from the source and destination $\beta = 0$ dB, and close to source $\beta = 30$ dB.

Table 4.1 Optimum power allocation values for APA (BPSK)

SNR [dB]	$\beta = -30dB$	$\beta = 0dB$	$\beta = 30dB$
	Λ	Λ	Λ
5	0.9764	0.6598	0.5020
10	0.9764	0.6634	0.5006
15	0.9764	0.6647	0.4996
20	0.9764	0.6651	0.4996
25	0.9764	0.6653	0.4995
30	0.9764	0.6653	0.4995
35	0.9764	0.6653	0.4995
40	0.9764	0.6653	0.4995

Table 4.2 Optimum power allocation values for APA (QPSK)

SNR [dB]	$\beta = -30dB$	$\beta = 0dB$	$\beta = 30dB$
	Λ	Λ	Λ
5	0.9776	0.6578	0.5030
10	0.9768	0.6621	0.5012
15	0.9765	0.6642	0.5001
20	0.9764	0.6650	0.4997
25	0.9764	0.6652	0.4996
30	0.9764	0.6653	0.4995
35	0.9764	0.6653	0.4995
40	0.9764	0.6653	0.4995

Table 4.3 Optimum power allocation values for APA (16-PSK)

SNR [dB]	$\beta = -30dB$	$\beta = 0dB$	$\beta = 30dB$
	Λ	Λ	Λ
5	0.9906	0.6598	0.5020
10	0.9842	0.6634	0.5506
15	0.9764	0.6647	0.4996
20	0.9774	0.6651	0.4996
25	0.9776	0.6653	0.4995
30	0.9765	0.6653	0.4995
35	0.9765	0.6653	0.4995
40	0.9765	0.6653	0.4995

Table 4.4 Optimum power allocation values for APA (16-QAM)

SNR [dB]	$\beta = -30dB$	$\beta = 0dB$	$\beta = 30dB$
	Λ	Λ	Λ
5	0.9860	0.6716	0.5061
10	0.9813	0.6603	0.5046
15	0.9793	0.6628	0.5027
20	0.9787	0.6652	0.5014
25	0.9785	0.6662	0.5008
30	0.9784	0.6665	0.5006
35	0.9784	0.6666	0.5005
40	0.9784	0.6666	0.5005

From Tables (4.1-4.4), we observe that when the source is close to the destination optimum values of Λ are ~ 0.95. These values indicate that it is efficient to spend most of power in the broadcast phase, the remaining power (i.e., $1-\Lambda$) should be dedicated to the relay. Similarly, when the relay is equidistant from source and destination nodes, the overall power in broadcasting phase, required to achieve minimum BER is $\Lambda \sim 66\%$. The power allocation in the broadcast phase continues to drop, when relay is near the source. In this case power allocation parameter is found to be $\Lambda \sim 0.5$.

In Figures 4.6, 4.7, 4.8, and 4.9, we demonstrate performance gains in power efficiency (as predicted by the derived Union bound) achieved by OPA over EPA for a target BER of 10^{-3}. From these figures, we observe that performance improvements up to 3db can be achieved for negative values of β (i.e., relay is close to destination) As relay moves from destination to source, the performance curves of EPA and OPA converges to each other. It is also noted here that for higher modulation schemes, the required SNR to achieve the same BER also increases.

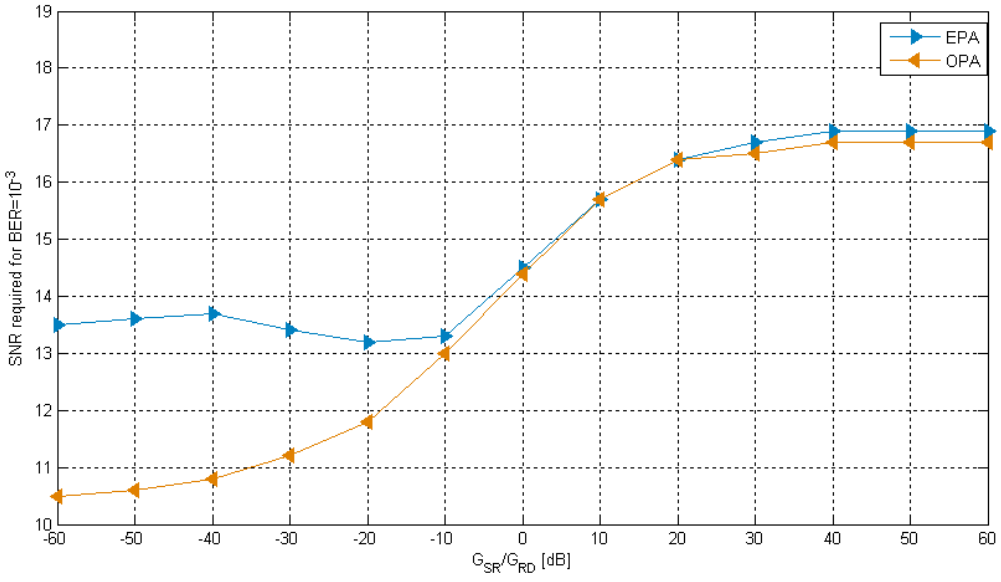

Figure 4.6 Power savings through OPA (BPSK)

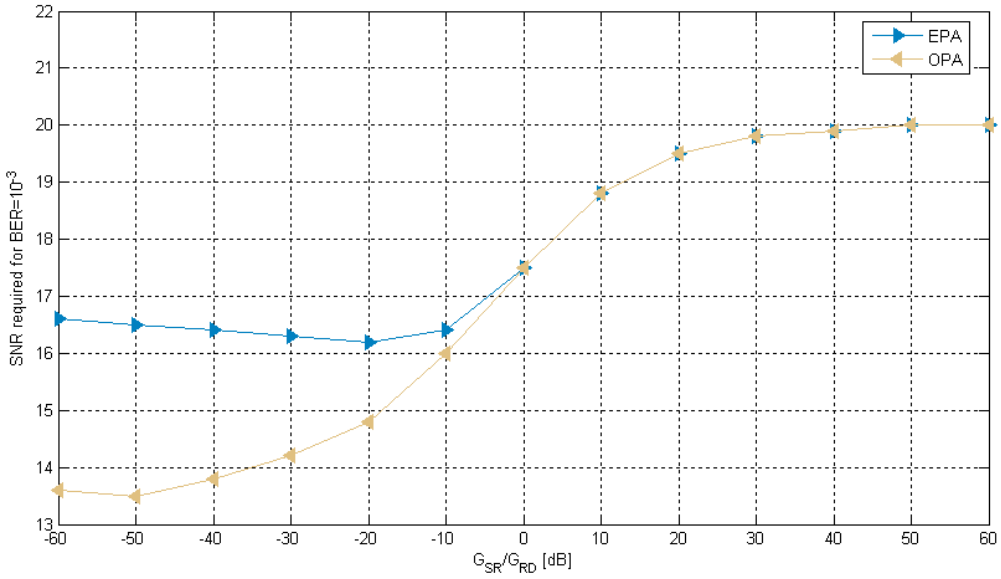

Figure 4.7 Power savings through OPA (QPSK)

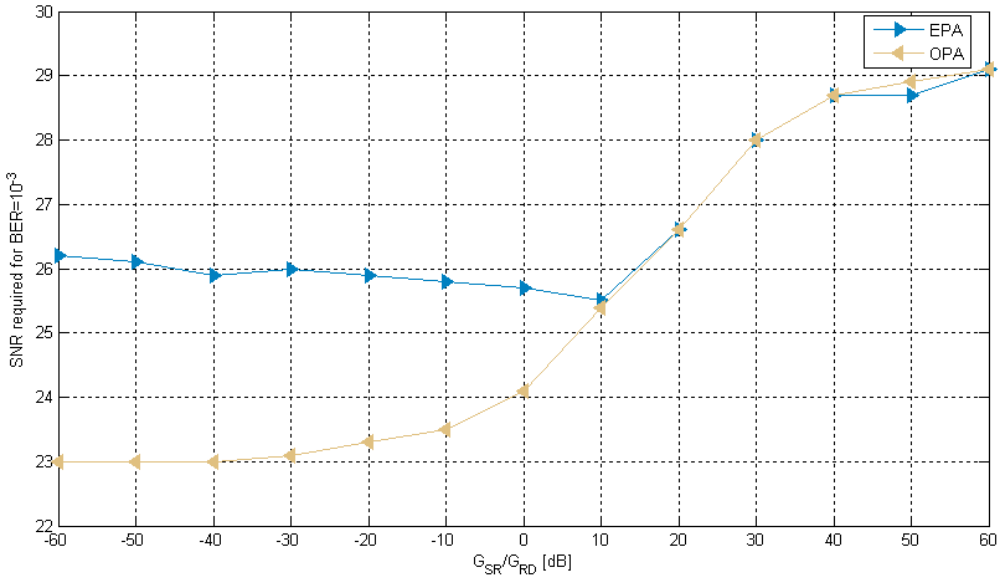

Figure 4.8 Power savings through OPA (16-PSK)

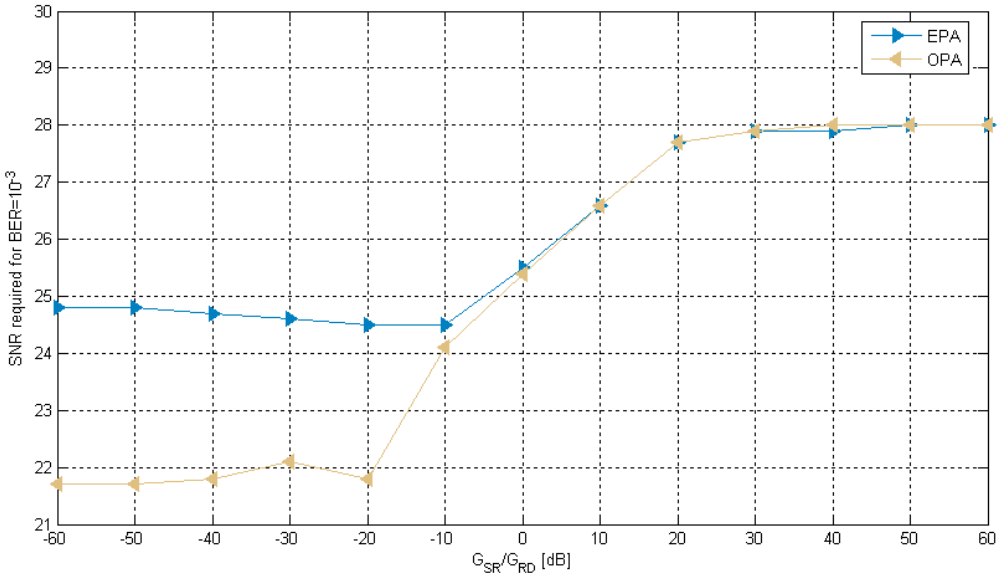

Figure 4.9 Power savings through OPA (16-QAM)

From the analysis of power gains, we observe that performance improvements up to 3dB can be achieved for negative values of β. Also, as the location of the relay is changed from near-destination to near-source, the performance curves of EPA and OPA converges to each other. It is also noted here that for higher m-PSK modulation schemes, the required SNR to achieve the same BER also increases.

4.2.2 Optimum Power Allocation (VA)

In Tables (4.5- 4.8), we present the optimum power allocation values for VA cooperative scheme assuming $\theta = \pi$, and path loss coefficient $\alpha = 2$ for different modulation schemes. For the purpose of clearly identifying the change trend of OPA values, we have considered $\beta = -30dB$, $\beta = 0dB$ and $\beta = 30dB$.

Table 4.5 Optimum power allocation for VA (BPSK)

SNR [dB]	$\beta = -30dB$	$\beta = 0dB$	$\beta = 30dB$
	Λ	Λ	Λ
5	0.9030	0.6660	0.5530
10	0.9460	0.6760	0.5350
15	0.9590	0.6770	0.5270
20	0.9620	0.6780	0.5240
25	0.9630	0.6780	0.5230
30	0.9630	0.6780	0.5230
35	0.9630	0.6780	0.5230
40	0.9630	0.6780	0.5230

Table 4.6 Optimum power allocation for VA (QPSK)

SNR [dB]	$\beta = -30dB$	$\beta = 0dB$	$\beta = 30dB$
	Λ	Λ	Λ
5	0.9720	0.6510	0.5990
10	0.9730	0.6730	0.5580
15	0.9730	0.6770	0.5410
20	0.9730	0.6780	0.5340
25	0.9730	0.6780	0.5320
30	0.9730	0.6780	0.5320
35	0.9730	0.6780	0.5310
40	0.9730	0.6780	0.5310

Table 4.7 Optimum power allocation for VA (16-PSK)

SNR [dB]	$\beta = -30dB$	$\beta = 0dB$	$\beta = 30dB$
	Λ	Λ	Λ
5	0.9280	0.6700	0.5530
10	0.9600	0.6840	0.5420
15	0.9690	0.6860	0.5360
20	0.9700	0.6910	0.5370
25	0.9710	0.6990	0.5370
30	0.9710	0.6970	0.5290
35	0.9710	0.6970	0.5290
40	0.9710	0.6970	0.5290

Table 4.8 Optimum power allocation for VA (16-QAM)

SNR [dB]	$\beta = -30dB$	$\beta = 0dB$	$\beta = 30dB$
	Λ	Λ	Λ
5	0.9640	0.6720	0.5630
10	0.9720	0.6900	0.5530
15	0.9710	0.6940	0.5420
20	0.9720	0.6930	0.5410
25	0.9720	0.6920	0.5400
30	0.9720	0.6920	0.5370
35	0.9720	0.6920	0.5360
40	0.9720	0.6910	0.5360

In VA scheme, when the source is close to the destination optimum values of Λ are ~ 0.97. For β=0dB, the optimum values changes in the range of $\sim$ 67%-69%, depending upon the type of modulation used. Similarly, when the relay is close to the source, the overall power in broadcasting phase, required to achieve minimum BER is in the range of $\Lambda \sim$ 53%-56%. This is slightly higher when compared to the same relay location in APA scheme

In Figures 4.10, 4.11, 4.12, and 4.13, we demonstrate performance gains in power efficiency (as predicted by the derived Union bound) achieved by OPA over EPA for a target BER of 10^{-3}. From these figures, we observe that performance improvements up to 3dB can be achieved for negative values of β (i.e., relay is close to destination). As relay moves from destination to source, the performance curves of EPA and OPA converges to each other. It is also noted here that for higher modulation schemes, the required SNR to achieve the same BER also increases

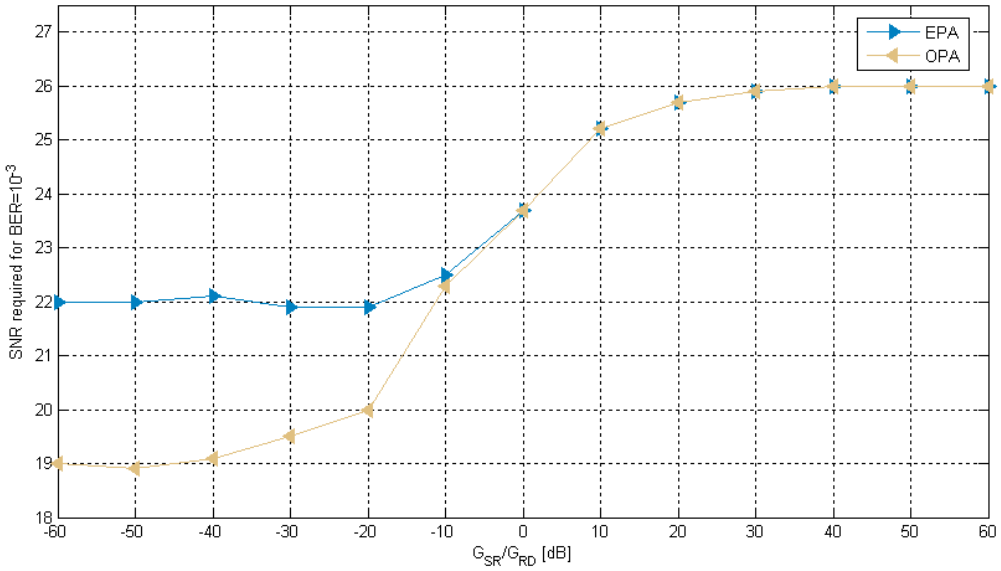

Figure 4.10 Power savings through OPA (BPSK)

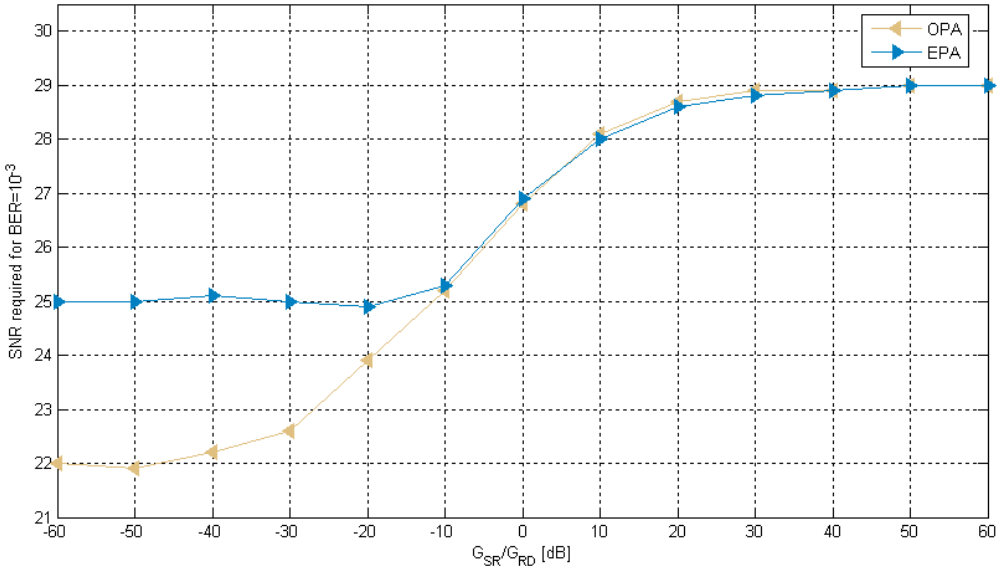

Figure 4.11 Power savings through OPA (QPSK)

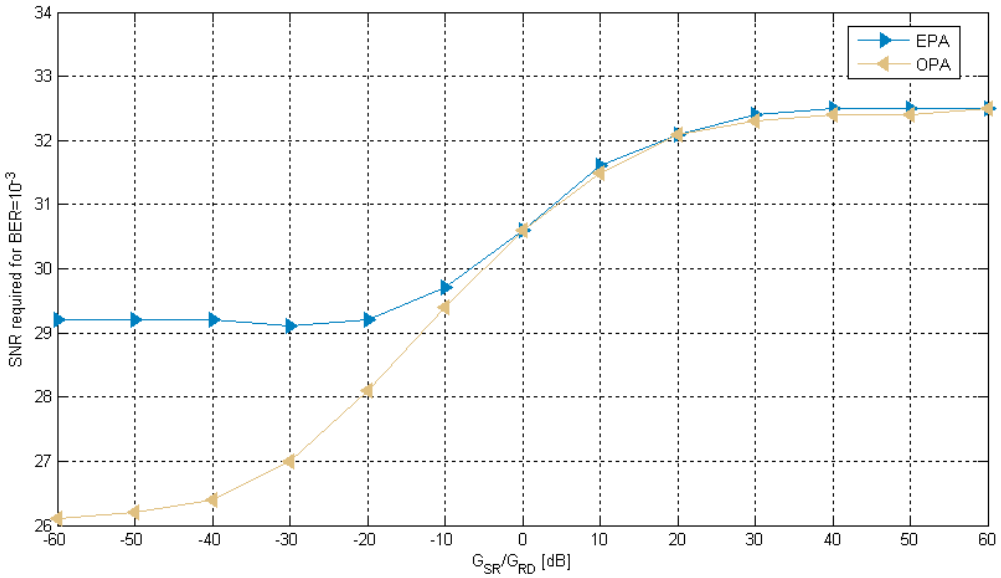

Figure 4.12 Power savings through OPA (16-PSK)

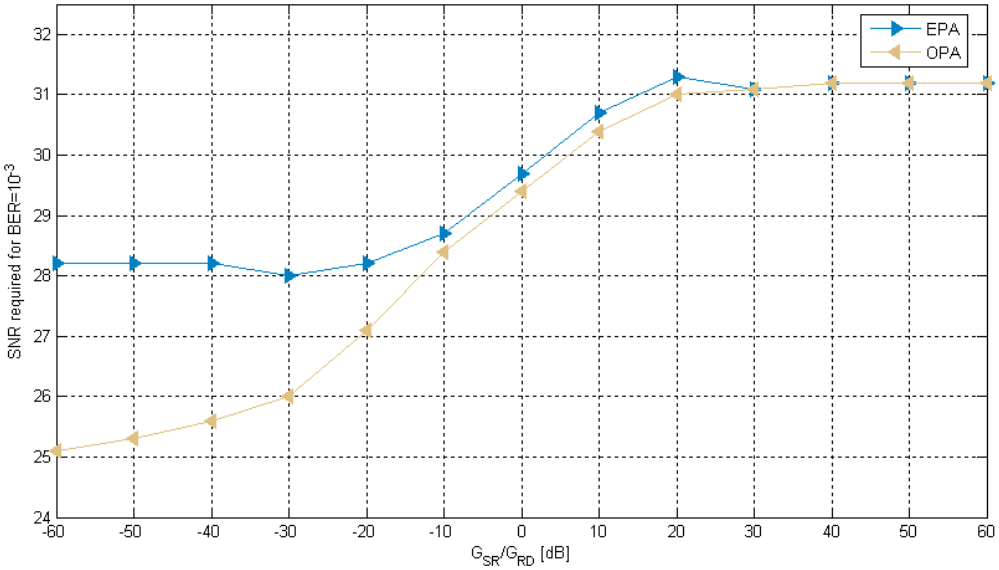

Figure 4.13 Power savings through OPA (16-QAM)

Chapter 5

SIMULATION RESULTS AND DISCUSSION

In this section we present the Monte-Carlo simulation results to elaborate on our analytical results in the previous section.

5.1 BER Performance of APA Cooperative Scheme

In Figures 5.1, 5.2, and 5.3 we compare the performance of simulated BER for APA, with equal power allocation and optimum power allocation. Here we have assumed $\theta = \pi$, and path-loss coefficient $\alpha = 2$. As a benchmark, we have also included the performance of non-cooperative direct transmission (i.e., no relaying), Alamouti scheme with two transmit antenna over cascaded fading channel, and MRC with two receive antennas over cascaded fading channels. In order to make a fair comparison in terms of throughput rate, benchmark schemes are simulated with BPSK and cooperative scheme with QPSK, to achieve the same rate.

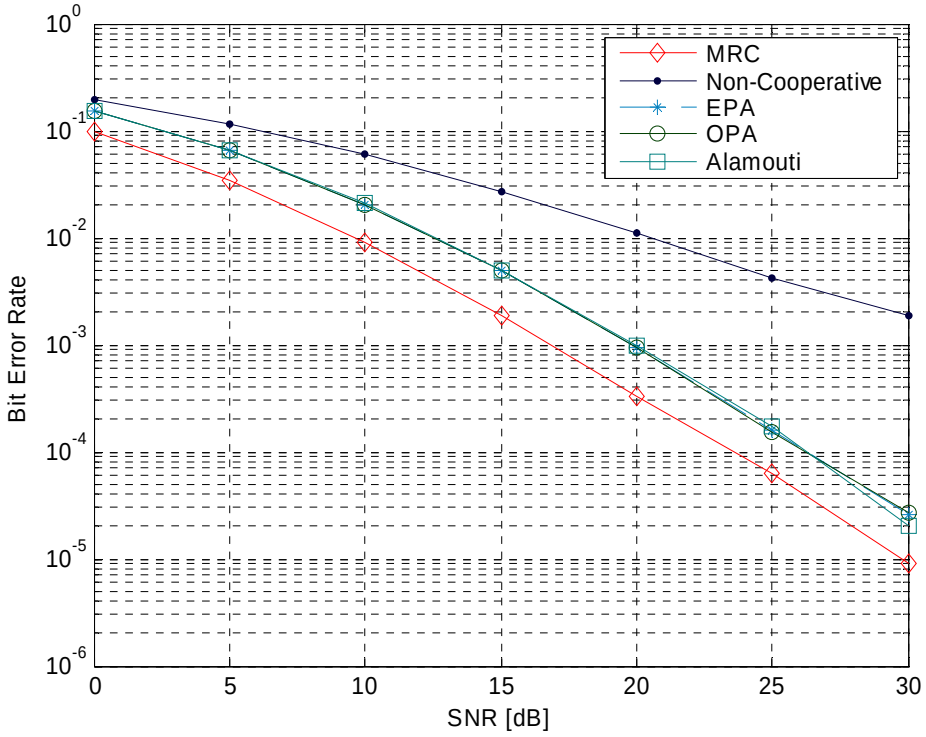

Figure 5.1 Performance results for APA with $\beta = 30$dB

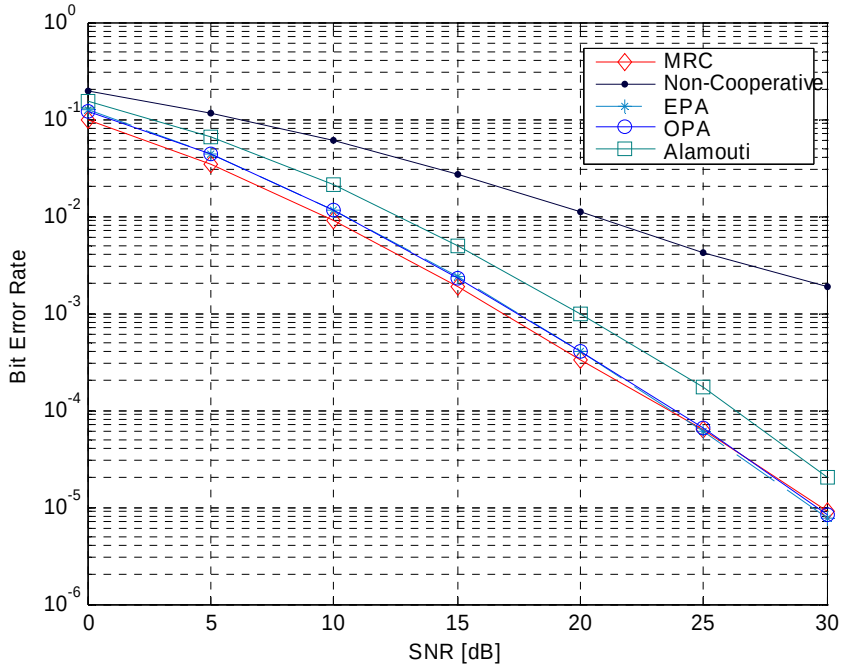

Figure 5.2 Performance results for APA with $\beta = 0$dB

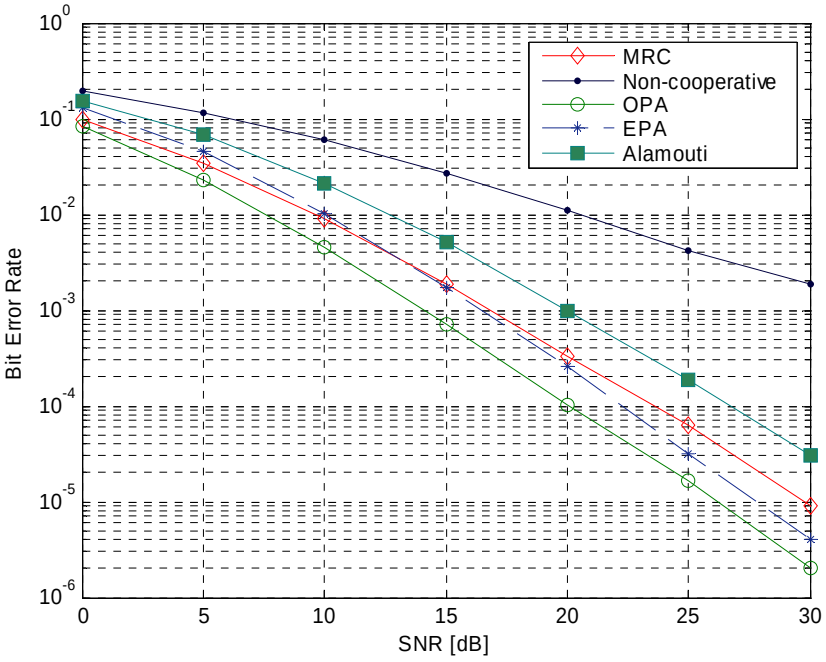

Figure 5.3 Performance results for APA with $\beta = -30$dB

As observed from above figures, the largest performance gain through OPA is obtained when relay is moved close to the destination. Specifically, for β = -30dB, we see a performance improvement of 2.8dB at BER of10^{-3}. This confirms our earlier observation on the analytical results where performance improvement of 3dB is predicted (see Figure 4.9). For this particular relay location, we also observe that performance of OPA outperforms MRC by 2.7dB. This is expected because in MRC both independent links encounter cascaded Rayleigh fading, but in APA only source-to-destination link experiences cascaded Rayleigh. For other locations, the performance gains through OPA are less and its performance is comparable to that of MRC for β = 0dB and less than that for β = 30dB

To demonstrate the effect of constellation size, we now simulate BER performance of OPA and EPA considering higher modulation schemes in Figures (5.4-5.6). The cooperative schemes are now simulated with 16-PSK and 16-QAM while the benchmark schemes are simulated with QPSK.

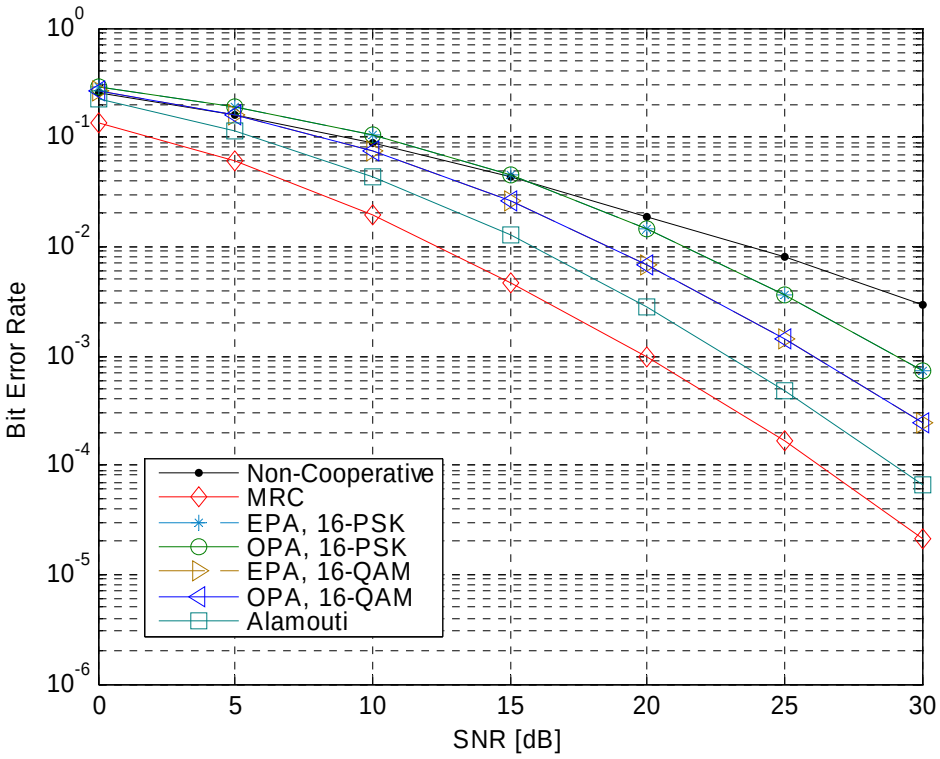

Figure 5.4 Performance results for APA with β = 30dB

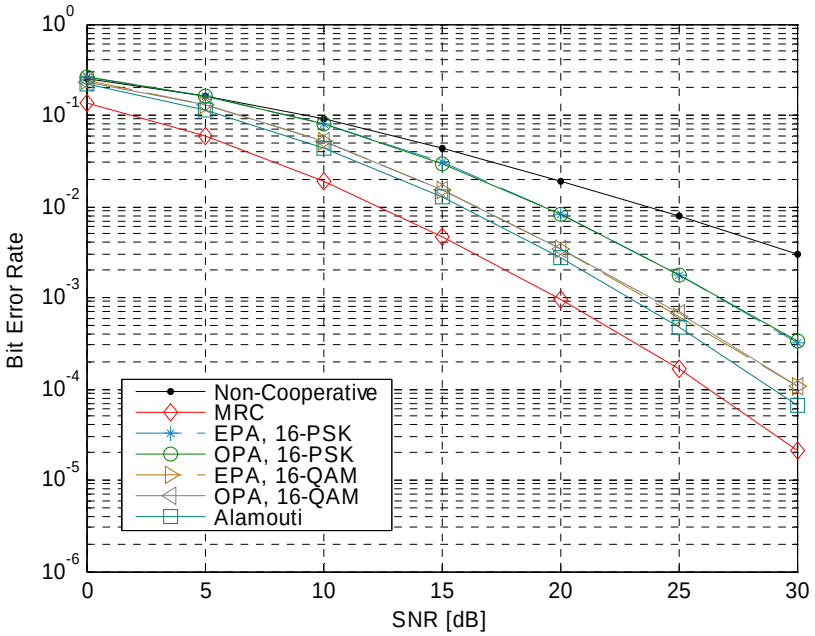

Figure 5.5 Performance results for APA with $\beta = 0$db

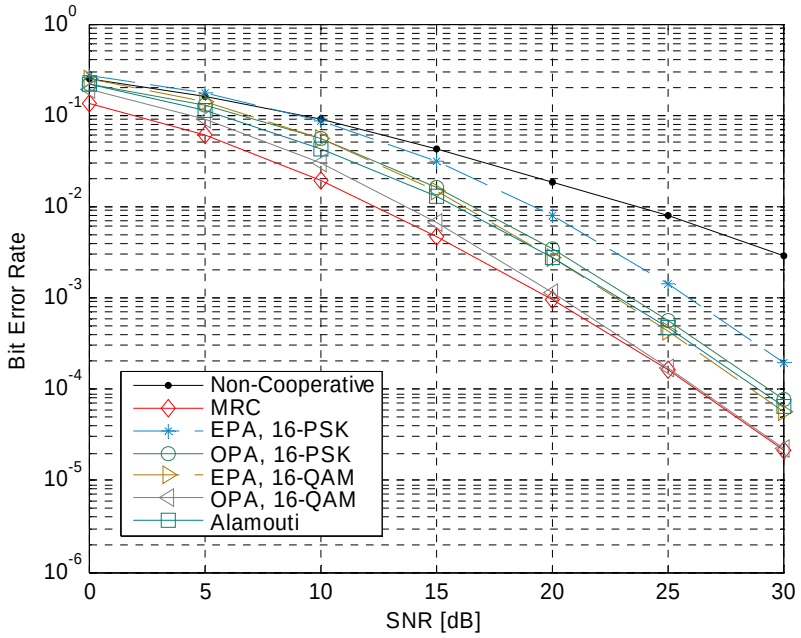

Figure 5.6 Performance results for APA with $\beta = -30$dB

With higher modulations OPA still outperforms EPA by 2.8dB when relay is close to destination. An interesting observation over here is that with higher modulation schemes the OPA does not outperforms the MRC. This shows the effect of crowded nature of signal constellations under consideration. Also the comparison between 16-PSK and 16-QAM confirms the better performance of QAM scheme due to the larger minimum distance.

5.2 BER Performance of VA

In Figures 5.7, 5.8, and 5.9 we compare the performance of simulated BER for VA cooperative scheme, with equal power allocation and optimum power allocation. Here we assume $\theta = \pi$, and path-loss coefficient $\alpha = 2$. As a benchmark, we have also included the performance of non-cooperative direct transmission (i.e., no relaying), Alamouti scheme with two transmit antenna over cascaded fading channel, and MRC with two receive antennas over cascaded fading channels. In order to make a fair comparison in terms of throughput rate, benchmark schemes are simulated with BPSK and cooperative scheme with QPSK, to achieve the same rate.

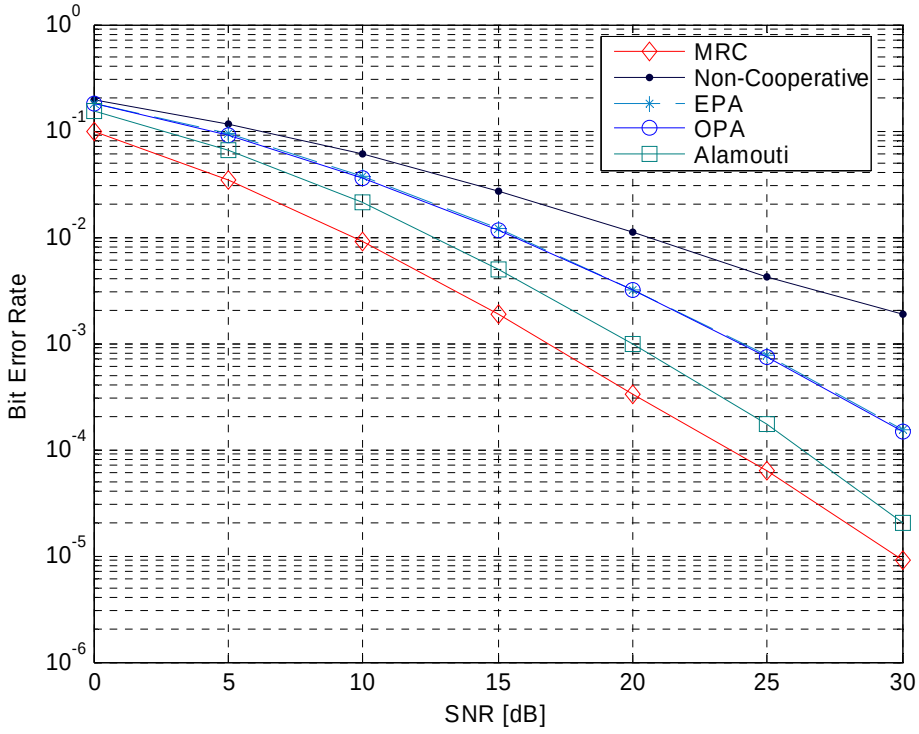

Figure 5.7 Performance results for VA with $\beta = 30$dB

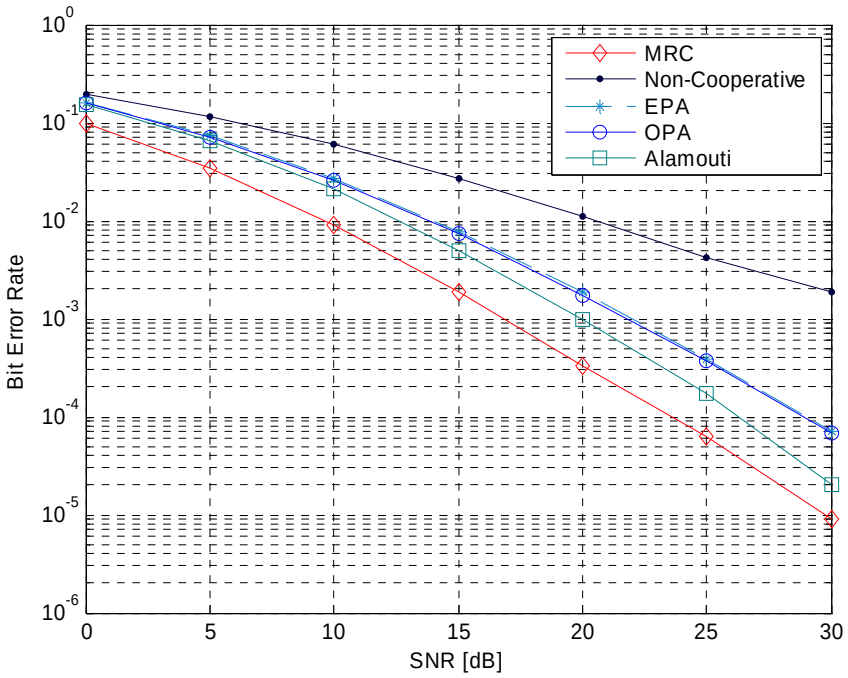

Figure 5.8 Performance results for VA with $\beta = 0$dB

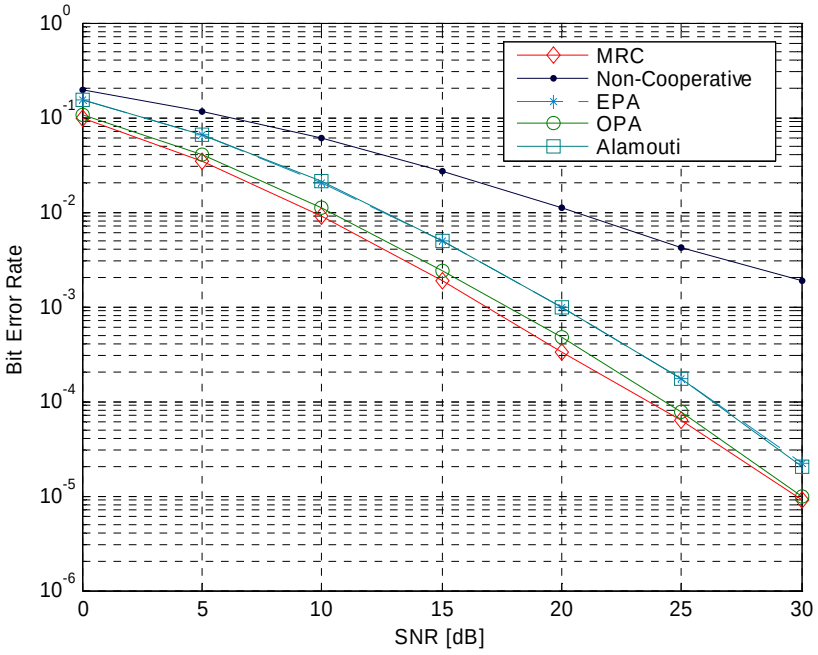

Figure 5.9 Performance results for VA with $\beta = -30$dB

As observed from above figures, the most significant performance gain through OPA is obtained when relay is moved close to the destination. Specifically, for β = -30dB, we see a performance improvement of 2.1dB at BER of10^{-3}. For this particular relay location, we also observe that performance of OPA is slightly away from that of MRC scheme. In contrast to AP scheme, for the relay location β = -30dB the performance of OPA does not out performs MRC. This is because now in MRC and VA cooperative scheme all links are cascaded Rayleigh.

To demonstrate the effect of constellation size, we simulated BER performance of OPA and EPA considering higher modulation schemes in Figures 5.4, 5.5, and 5.6. The cooperative schemes are now simulated with 16-PSK and 16-QAM while the benchmark schemes are simulated with QPSK

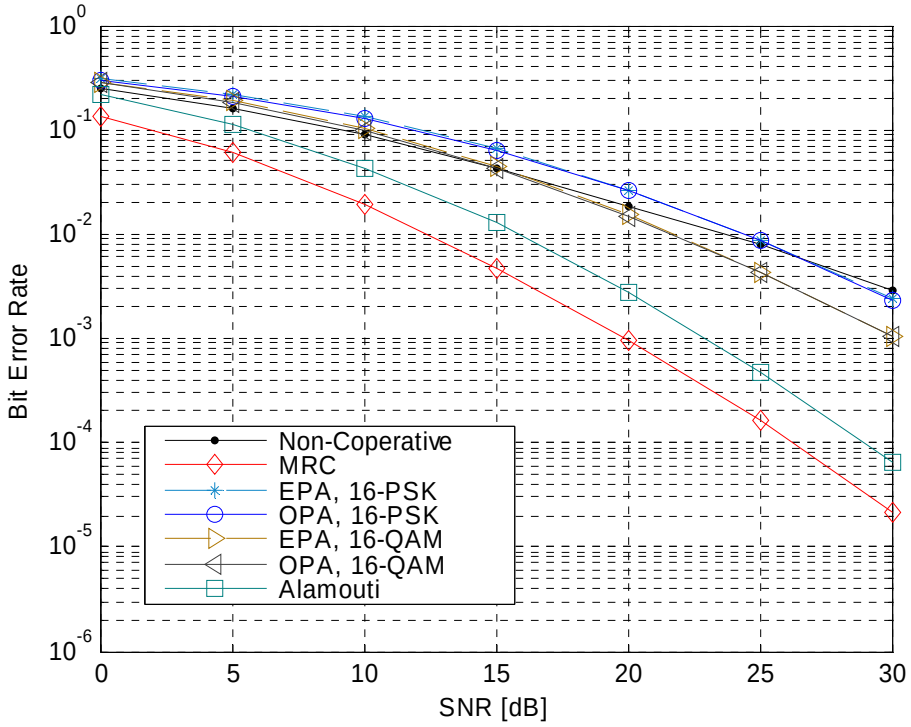

Figure 5.10 Performance results for VA with β = 30dB

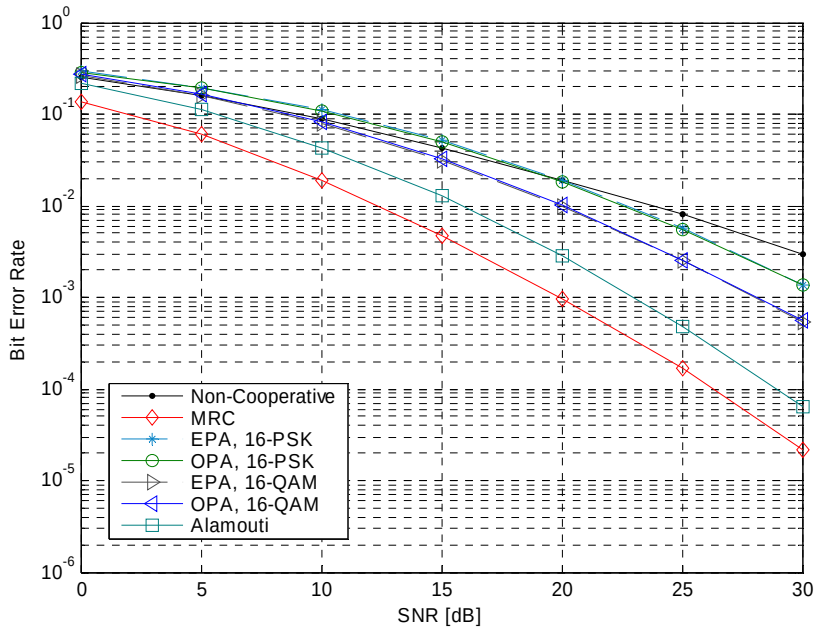

Figure 5.11 Performance results for VA with $\beta = 0$dB

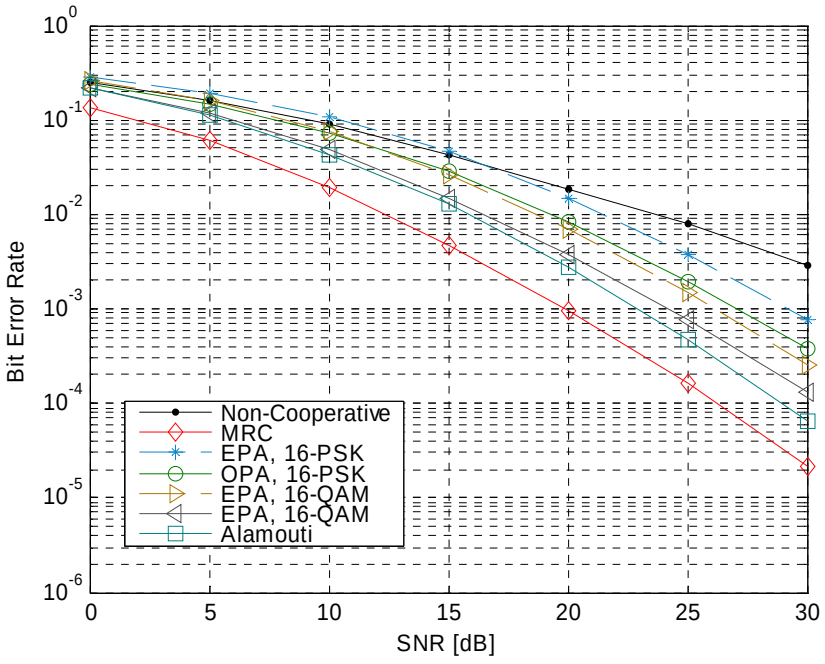

Figure 5.12 Performance results for APA with $\beta = -30$dB

With higher modulations OPA still outperforms EPA by 2.8dB when relay is close to destination. The performance improvement observed when relay is close to destination and 16-QAM modulation used, is comparable to Alamouti scheme. This indicated the degradation in performance when compared to same scenario in APA. Similarly, to APA, the performance of 16-QAM is slightly better than 16-PSK

Chapter 6

Conclusions

Cascaded Rayleigh fading is a realistic channel model for vehicular environments. Realizing the sparseness on this particular channel model, this thesis has analyzed and optimized the performance of APA and VA cooperative schemes over cascaded Rayleigh channel. The main summary and main findings of this thesis are reported below

In Chapter 2, we presented our system transmission model. We have provided a detailed description of our channel model under consideration. We followed it up with a comprehensive analysis of our transmission model for single-relay cooperative scheme.

In Chapter 3, derivation of PEP expressions for each inter-vehicular scheme (APA &VA) was presented. Through the derivation of PEP, we found that the asymptotical diversity order is two. Although this is only partially extracted in practical SNR range due to the nature of underlying cascaded Rayleigh fading.

In Chapter 4, we derived union bounds on BER. Based on the derived BER expressions, we formulated power allocation problem and determined optimum power allocation values in the sense of minimizing BER. Performance gains up to 3.2dB at a target BER of 10^{-3} have been observed depending upon the relay location and modulation scheme. Our results further demonstrated that OPA provides significant performance improvement in particular for cases when relay is located close to destination.

In Chapter 5, extensive Monte-Carlo simulation study of APA and VA cooperative schemes were carried out. Our simulation results validated the power savings as predicted by OPA. In this chapter, we further presented the performance comparisons of cooperative schemes and non-cooperative direct transmissions. In general, we observed that the performance of M-PSK degrades as we move toward higher order modulation. When considering higher modulation schemes, the performance of APA approaches to MRC, using optimum values. Whereas, in VA the maximum performance improvement is comparable to Alamouti scheme.

Bibliography

[1] M. Sauter, *Communication Systems for the Mobile Information Society*, John Wiley & Sons, 2006.

[2] M. Sun, W. Feng, T. Lai, K. Yamada, H. Okada, and K. Fujimura, "GPS-based message broadcasting for inter-vehicular communication," in *Proc. of ICPP*, pp. 279-286, 2000.

[3] M. Oliphant, "The Mobile Phone Meets the Internet," *IEEE Spectrum*, pp. 20-28, August 1999.

[4] D. Reichardt, M. Miglietta, L. Moertti, P. Morsink, and W. Schulz, "CarTALK 2000-safe and comfortable driving based upon inter-vehicle communication," in *Proc. IEEE Intelligent Vehicle Symposium (IV'02*), 2002.

[5] DSRC, *Dedicated Short Range Communications*, grouper.ieee.org/groups/scc32/dsrc

[6] I. Stojemenovic, "Position-based routing in ad hoc networks," *IEEE Comm. Magazine*, vol. 40(7), pp. 138-134, 2002.

[7] O. Gehring and H. Fritz, "Practical results of a longitudinal control concept for truck platooning with vehicle to vehicle communication," in *Proc IEEE Intelligent Transportation System (ITSC'97)*, pp 117-122, 1997

[8] J. K. Hedrick, M. Tomizuka, and P. Varaiva, "Control issue in automated highway systems," *IEEE Control System Magazine*, vol. 14(6), pp. 21-32, 1997

[9] Z. Yunpeng L. Stibor, B. Walke, J- H. Reumerman, A. Barroso, "A Novel MAC Protocol for Throughput Sensitive Applications in Vehicular Environments," *IEEE Vehicular Technology Conf. (VTC 2007*), pp. 2580-2584, April, 2007.

[10] J. Luo and J- P. Hubaux, "A Survey of Inter-Vehicle Communication," *IC Technical Report*, 24, 2004

[11] J. N. Laneman and G. W. Wornell, "Distributed space-time coded protocols for exploiting cooperative diversity in wireless networks," *IEEE Trans. Inform, Theory*, vol. 49(10), pp. 2415-2525, Oct, 2003

[12] A. Sendonaris, E. Erkip, and B. Aazhang, "User cooperation diversity Part I: system description," *IEEE Trans. Commun*., vol. 51(11), pp. 1927-1938, Nov., 2003

[13] R. U. Nabar, H. Boelcskei, and F. W. Kneubhueler, "Fading relay channels: Performance limits and space-time signal design," *IEEE Journal on Selected Areas in Communications*, vol 22, pp. 1099-1109, Aug. 2004

[14] T. S. Rappaport, *Wireless Communications: Principles and Practice*, Prentice Hall PTR, 2000.

[15] V. Kuhn, *Wireless Communications Over MIMO Channel : Applications to CDMA and Multiple Antennas*, Wiley, 2006.

[16] J. G. Proakis*, Digital Communications*, 2nd ed., New York: McGraw-Hill, 1989A.

[17] P. Stavroulakis, "Interference Analysis of Communications Systems," *IEEE Press*, New York, 1980.

[18] E. Shim, and N. Safari, "A simple theoretical model for polarization diversity reception in wireless environments," *IEEE Int. Symp. Antenna and Propagations Society, v*ol. 2, pp. 1332-1335, 1999

[19] S. M. Alamouti, "Simple transmit diversity technique for wireless communications," *IEEE Journal on Select Areas in Communications*, vol. 16, pp. 1451-1458, 1998

[20] J. G. Foschini, "Layered space-time architecture for wireless communication in a fading environment when using multi element antennas," *Bell Labs Tech. J.*, vol2, pp. 41-59, Autumn 1996

[21] J. G. Foschini Jr., D. G. Golden , A. R. Valenzuela and W.P. Wolniansky, "Simplified processing for high spectral efficiency wireless communication employing multi-element arrays," *IEEE Journal on Selected Area in Communications*, vol. 17, pp. 1841-1852, Nov 1999.

[22] E. G. Larsson and P. Stoica, *Space-Time Block Coding for Wireless Communications*, Cambridge University Press, June 2003

[23] A. Wittneben, "Base station modulation diversity for digital SIMULCAST," in *IEEE Vehicular Technology Conf.,* pp. 848-853, May 1991

[24] A. Wittneben, "A new bandwidth efficient transmit antenna modulation diversity scheme for linear digital modulation," in *IEEE International Conf. Communications*, pp. 1630-1634, May 1993

[25] J. H. Winter, "The diversity gain of transmit diversity in wireless system with Rayleigh fading," *IEEE Int. Conf. Communications*, pp. 1121-1125, 1994

[26] V. Tarokh, N. Seshadri, and A. R. Calderbank, "Space-time codes for high data rates wireless communications: Performance criterion and code construction," *IEEE Trans. Inform. Theory*, vol. 44, pp. 744-765, 1998

[27] A. Paulraj, D. Gore and R. Nabar, *Introduction to Space-Time Wireless Communications*, Cambridge University Press, May 2003

[28] J. N. Laneman, G. W. Wornell, and D. N. C. Tse, "An Efficient Protocol for Realizing Cooperative Diversity in Wireless Networks," in *IEEE Int. Symp. Info. Theory*, Washington, DC, June 2001

[29] T. M. Cover and A. A. El Gamal. "Capacity theorems for the relay channel," *IEEE Trans. Inform. Theory*, vol. 25, pp. 572-584, Sept. 1979

[30] J. N. Laneman, D. N. C. Tse, and G. W. Wornell, "Cooperative Diversity in Wireless Networks: Efficient Protocols and Outage Behavior," to appear in *IEEE Trans. Inform. Theory*

[31] V. Tarokh, H. Jafarkhani, and A.R. Calderbank, "Space-time block coding from orthogonal designs," *IEEE Trans. Inform. Theory*, vol. 45, pp. 1456-1467, 1999.

[32] H. Wang and X.-G. Xia, "Upper bounds of rates of complex orthogonal space-time block codes," *IEEE Trans. Inf. Theory*, vol. 49, no. 10, pp. 2788–2796, October, 2006

[33] S. Das, N. Al-Dhahir, and R. Calderbank, "Novel full-diversity high-rate STBC for 2 and 4 transmit antennas," *IEEE Commun. Lett.,* vol. 10, no. 3, pp. 171-173, March 2006.

[34] H. Ochiai, P. Mitran, and V. Tarokh, "Variable-Rate Two-Phase Collaborative Communication Protocols for Wireless Networks", *IEEE Trans. Inf. Theory*, vol. 52, Issue 9, pp., 4299 – 4313, Sept. 2006.

[35] H. Mheidat and M. Uysal "Impact of Receive Diversity on the Performance of Amplify-and-Forward Relaying under APS and IPS Power Constraints", *IEEE Commun. Lett.,* vol. 10, no. 6, p. 468-470, June 2006

[36] M. M. Fareed and M. Uysal, "Optimum Power Allocation for Fading Relay Channels", *IEEE VTC'07-Fall*, Baltimore, Maryland, USA, September 2007

[37] I. Z. Kovacs, " Radio Channel Characterization for Private Mobile Radio Systems: Mobile-to-mobile radio link investigation," *PhD Thesis*, Aalborg University, Sep, 2002

[38] G.A.Zajic, and L.G. Stuber, "Simulation Models for MIMO Mobile-to-Mobile Channels," in *Proc. Of Military Communications Conference,* Oct, 2006

[39] A.S. Akki and F.Haber, " A Statistical Model of Mobile-to-Mobile Communication Channel," *IEEE Trans. Vehicular Tech.*, vol. 35(1), pp.2-7, Feb., 1986

[40] W. Honcharenko, H. L. Bertoni, and J. L. Dailing, "Bilateral Averaging Over Receiving and Transmitting Areas for Accurate Measurements of Sector Average Signal Strength Inside Buildings," *IEEE Trans. Antennas and Propagation*, vol. 43(5), pp. 508-512, May, 1997

[41] V. Ercerg, S. J. Fortune, J. Ling, and R. A. Valenzuela, "Comparison of a Computer Based Propagation Toll with Experimental Data Collected in Urban Microcellular Environments," *IEEE Journal on Selected Areas in Commun*. vol. 15(4), pp. 677-684, May, 1997

[42] J.P.M.G. Linnartz (Ed), *Wireless Communication, The Interactive Multimedia CD-ROM*, Kluwer Academics, NY. 2001

[43] J. Salo, H. M. El-Sallabi and P. Vainikainen, "The distribution of the product of independent Rayleigh random variables", *IEEE Trans. On Antennas and Propagation,* vol. 54(2), Sept. 2006.

[44] L. C. Andrews, *Special Functions of Mathematics for Engineers*, Second Edition, McGraw-Hill, Inc., NY, 1985.

[45] M. Uysal, "Diversity Analysis of Space-Time Coding in Cascaded Rayleigh Fading Channels", *IEEE Commun Lett.*, vol. 10(3), pp. 165-167, Mar. 2006

[46] G. K. Karagiannidis, T. A. Tsiftsis and R. K. Mallik, "Bounds of Multihop Relayed Communications in Nakagami-m Fading", *IEEE Trans. Commun*, vol. 54, pp. 18-22, Jan., 2006

[47] V. Tarokh, N. Seshadri, A. Calderbank, "Space-time codes for high data rate wireless communication: Performance criterion and code construction", *IEEE Trans. Inf. Theory*, vol. 44(2), pp. 744-765, Mar. 1998.

[48] I. S. Gradshteyn and I. M. Ryzhik, *Table of Integrals, Series and Products*, Academic Press, 5th ed, 1994

[49] A. Papoulis, *Probability, Random Variables and Stochastic Processes,* Second Edition, McGraw-Hill, NY, 1984.

[50] S. Benedetto and E. Biglieri, *Principles of Digital Transmission with Wireless Applications*, Kluwer Academic, NY, 1999

[51] A. Host-Madsen and J. Zhang, "Capacity bounds and power allocation in wireless relay channel," *IEEE Trans. Information Theory*, vol.51, pp. 2020-2040, Jun, 2005

[52] N. Ahmed and B. Aazhang, “Outage minimization with the limited feedback for the fading relay channel,” *IEEE Trans. Communications*, vol.54, pp. 659-670, Apr., 2006

[53] M. O. Hasna and M. S. Alouini, ”Optimum power allocation for relayed transmissions over Rayleigh fading channels,” *IEEE Trans. Wireless Communications*, vol.3, pp. 1999-2004, Nov, 2004

.